

ISL88731A

SMBus Level 2 Battery Charger

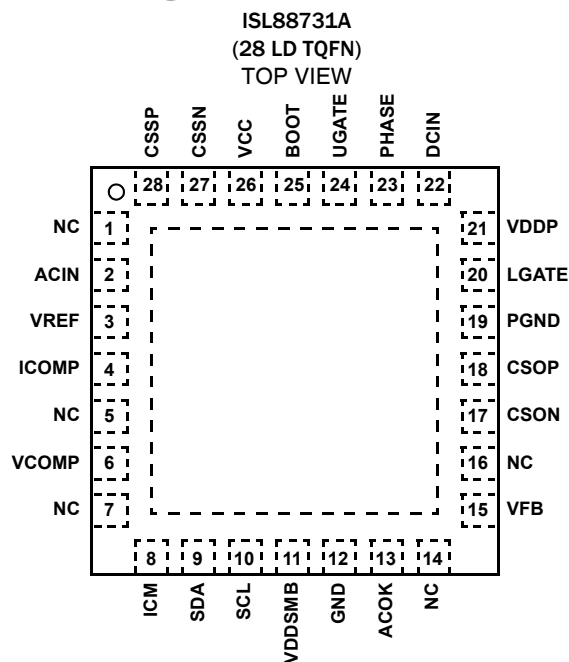
FN6738  
Rev 3.00  
June 8, 2011

The ISL88731A is a highly integrated Lithium-ion battery charger controller, programmable over the SMBus system management bus (SMBus). The ISL88731A is intended to be used in a smart battery charger (SBC) within a smart battery system (SBS) that throttles the charge power such that the current from the AC-adapter is automatically limited. High efficiency is achieved with a DC/DC synchronous-rectifier buck converter, equipped with diode emulation for enhanced light load efficiency and system bus boosting prevention. The ISL88731A charges one to four Lithium-ion series cells, and delivers up to 8A charge current. Integrated MOSFET drivers and bootstrap diode result in fewer components and smaller implementation area. Low offset current-sense amplifiers provide high accuracy with 10mΩ sense resistors. The ISL88731A provides 0.5% end-of-charge battery voltage accuracy.

The ISL88731A provides a digital output that indicates the presence of the AC-adapter as well as an analog output which indicates the adapter current within 4% accuracy.

The ISL88731A is available in a small 5mmx5mm 28 Ld thin (0.8mm) QFN package. An evaluation kit is available to reduce design time. The ISL88731A is available in Pb-Free packages.

Pin Configuration



Features

- 0.5% Battery Voltage Accuracy
- 3% Adapter Current Limit Accuracy
- 3% Charge Current Accuracy
- SMBus 2 Wire Serial Interface
- Battery Short Circuit Protection
- Fast Response for Pulse-Charging
- Fast System-Load Transient Response
- Monitor Outputs
  - Adapter Current (3% Accuracy)
  - AC-Adapter Detection
- 11-Bit Battery Voltage Setting
- 6 Bit Charge Current/Adapter Current Setting
- 8A Maximum Battery Charger Current
- 11A Maximum Adapter Current
- +8V to +28V Adapter Voltage Range
- Pb-Free (RoHS compliant)

Applications

- Notebook Computers
- Tablet PCs
- Portable Equipment with Rechargeable Batteries

Ordering Information

PART NUMBER (Notes 1, 2, 3)	PART MARKING	TEMP RANGE (°C)	PACKAGE (Pb-Free)	PKG. DWG. #
ISL88731AHRZ	ISL887 31AHRZ	-10 to +100	28 Ld 5x5 TQFN	L28.5x5B

NOTES:

1. Add "-T\*" suffix for tape and reel. Please refer to [TB347](#) for details on reel specifications.
2. These Intersil Pb-free plastic packaged products employ special Pb-free material sets, molding compounds/die attach materials, and 100% matte tin plate plus anneal (e3 termination finish, which is RoHS compliant and compatible with both SnPb and Pb-free soldering operations). Intersil Pb-free products are MSL classified at Pb-free peak reflow temperatures that meet or exceed the Pb-free requirements of IPC/JEDEC J STD-020.
3. For Moisture Sensitivity Level (MSL), please see device information page for [ISL88731A](#). For more information on MSL please see techbrief [TB363](#).

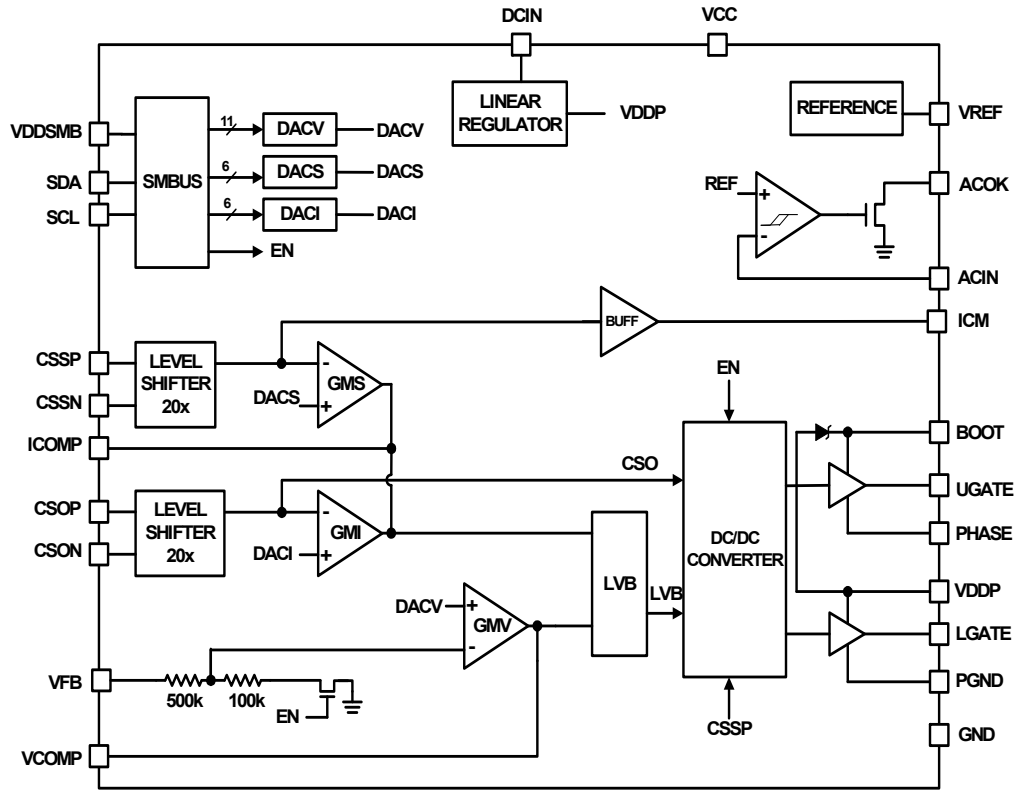


FIGURE 1. FUNCTIONAL BLOCK DIAGRAM

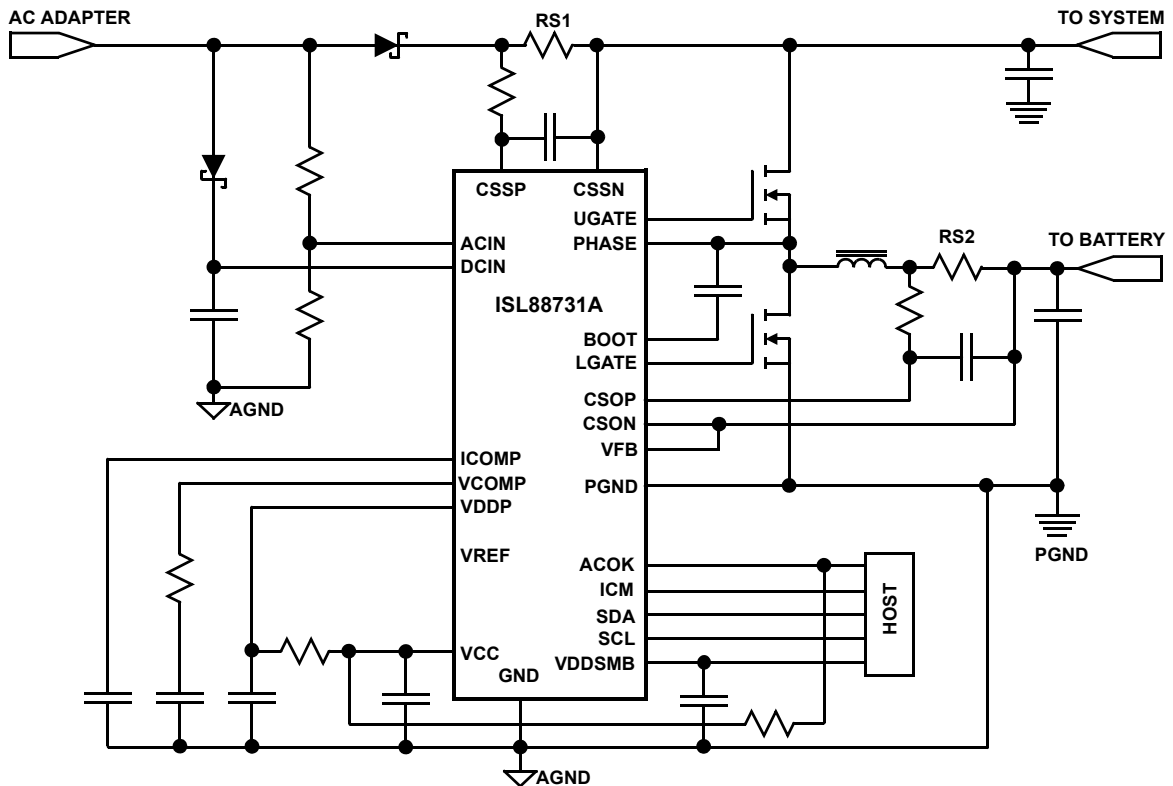


FIGURE 2. TYPICAL APPLICATION CIRCUIT

## Absolute Maximum Ratings

DCIN, CSSP, CSSN, CSOP, CSON, VFB	-0.3V to +28V
CSSP-CSSN, CSOP-CSON, PGND-GND	-0.3V to +0.3V
PHASE to GND	-6V to +30V
BOOT to GND	-0.3V to +33V
BOOT to PHASE	-0.3V to +6V
UGATE	PHASE - 0.3V to BOOT +0.3V
LGATE	.PGND - 0.3V to VDDP +0.3V
ICOMP, VCOMP, VREF, to GND	-0.3V to VCC +0.3V
VDDSMB, SCL, SDA, ACIN, ACOK	-0.3V to +6V
VDDP, ICM, VCC to GND, VDDP to PGND	-0.3V to +6V

## Thermal Information

Thermal Resistance (Typical, Notes 4, 5)	$\theta_{JA}$ ( $^{\circ}\text{C}/\text{W}$ )	$\theta_{JC}$ ( $^{\circ}\text{C}/\text{W}$ )
QFN Package	36	6
Junction Temperature Range	-55 $^{\circ}\text{C}$ to +150 $^{\circ}\text{C}$	
Operating Temperature Range	-10 $^{\circ}\text{C}$ to +100 $^{\circ}\text{C}$	
Storage Temperature	-65 $^{\circ}\text{C}$ to +150 $^{\circ}\text{C}$	
Pb-Free Reflow Profile	see link below	
	<a href="http://www.intersil.com/pbfree/Pb-FreeReflow.asp">http://www.intersil.com/pbfree/Pb-FreeReflow.asp</a>	

**CAUTION:** Do not operate at or near the maximum ratings listed for extended periods of time. Exposure to such conditions may adversely impact product reliability and result in failures not covered by warranty.

### NOTES:

- $\theta_{JA}$  is measured in free air with the component mounted on a high effective thermal conductivity test board with "direct attach" features. See Tech Brief [TB379](#)
- For  $\theta_{JC}$ , the "case temp" location is the center of the exposed metal pad on the package underside.

**Electrical Specifications** DCIN = CSSP = CSSN = 18V, CSOP = CSON = 12V, VDDP = 5V, BOOT-PHASE = 5.0V, GND = PGND = 0V, CVDDP = 1 $\mu\text{F}$ , IVDDP = 0mA,  $T_A$  = -10 $^{\circ}\text{C}$  to +100 $^{\circ}\text{C}$ . **Boldface limits apply over the operating temperature range, -10 $^{\circ}\text{C}$  to +100 $^{\circ}\text{C}$ .**

PARAMETER	CONDITIONS	MIN (Note 6)	TYP	MAX (Note 6)	UNITS
<b>CHARGE VOLTAGE REGULATION</b>					
Battery Full Charge Voltage and Accuracy	ChargeVoltage = 0x41A0	<b>16.716</b>	16.8	<b>16.884</b>	V
		<b>-0.5</b>		<b>0.5</b>	%
	ChargeVoltage = 0x3130	<b>12.529</b>	12.592	<b>12.655</b>	V
		<b>-0.5</b>		<b>0.5</b>	%
	ChargeVoltage = 0x20D0	<b>8.350</b>	8.4	<b>8.450</b>	V
		<b>-0.6</b>		<b>0.6</b>	%
ChargeVoltage = 0x1060	<b>4.163</b>	4.192	<b>4.221</b>	V	
	<b>-0.7</b>		<b>0.7</b>	%	
Battery Undervoltage Lockout Trip Point for Trickle Charge	VFB rising	<b>2.55</b>	2.7	<b>2.85</b>	V
Battery Undervoltage Lockout Trip Point Hysteresis		<b>100</b>	250	<b>400</b>	mV
<b>CHARGE CURRENT REGULATION</b>					
CSOP to CSON Full-Scale Current-Sense Voltage		<b>78.22</b>	80.64	<b>83.06</b>	mV
Charge Current and Accuracy	RS2 = 10m $\Omega$ (see Figure 2) ChargingCurrent = 0x1f80	<b>7.822</b>	8.064	<b>8.306</b>	A
		<b>-3</b>		<b>3</b>	%
	RS2 = 10m $\Omega$ (see Figure 2) ChargingCurrent = 0x0f80	<b>3.809</b>	3.968	<b>4.126</b>	A
		<b>-4</b>		<b>4</b>	%
	RS2 = 10m $\Omega$ (see Figure 2) ChargingCurrent = 0x0080	<b>64</b>	128	<b>220</b>	mA
		<b>-1.6</b>		<b>1.4</b>	%
Charge Current Gain Error	Based on charge current = 128mA and 8.064A	<b>-1.6</b>		<b>1.4</b>	%
CSOP/CSON Input Voltage Range		<b>0</b>		<b>19</b>	V

**Electrical Specifications**  $V_{DCIN} = V_{CSSP} = V_{CSSN} = 18V$ ,  $V_{CSOP} = V_{CSON} = 12V$ ,  $V_{DDP} = 5V$ ,  $V_{BOOT-PHASE} = 5.0V$ ,  $GND = PGND = 0V$ ,  $C_{VDDP} = 1\mu F$ ,  $I_{VDDP} = 0mA$ ,  $T_A = -10^\circ C$  to  $+100^\circ C$ . **Boldface limits apply over the operating temperature range,  $-10^\circ C$  to  $+100^\circ C$ .** (Continued)

PARAMETER	CONDITIONS	MIN (Note 6)	TYP	MAX (Note 6)	UNITS
Battery Quiescent Current	Adapter present, not charging, $I_{CSOP} + I_{CSON} + I_{PHASE} + I_{CSSP} + I_{CSSN} + I_{FB}$ $V_{PHASE} = V_{CSON} = V_{CSOP} = V_{DCIN} = 19V$ , $V_{ACIN} = 5V$		135	<b>400</b>	$\mu A$
	Adapter Absent $I_{CSOP} + I_{CSON} + I_{PHASE} + I_{CSSP} + I_{CSSN} + I_{FB}$ $V_{PHASE} = V_{CSON} = V_{CSOP} = 19V$ , $V_{DCIN} = 0V$	<b>-1</b>	0.2	<b>4</b>	$\mu A$
Adapter Quiescent Current	$I_{DCIN} + I_{CSSP} + I_{CSSN}$ $V_{ADAPTER} = 8V$ to $26V$ , $V_{BATTERY} 4V$ to $16.8V$		3	<b>10</b>	mA
<b>INPUT CURRENT REGULATION</b>					
CSSP to CSSN Full-Scale Current-Sense Voltage	$CSSP = 19V$	<b>106.7</b>	110	<b>113.3</b>	mV
Input Current Accuracy	$RS1 = 10m\Omega$ (see Figure 2) Adapter Current = <b>11004mA</b> or <b>3584mA</b>	<b>-3</b>		<b>3</b>	%
	$RS1 = 10m\Omega$ (see Figure 2) Adapter Current = <b>2048mA</b>	<b>-5</b>		<b>5</b>	%
Input Current Limit Gain Error	Based on InputCurrent = <b>1024mA</b> and <b>11004mA</b>	<b>-1.5</b>		<b>1.5</b>	%
Input Current Limit Offset		<b>-1</b>		<b>1</b>	mV
CSSP/CSSN Input Voltage Range		<b>8</b>		<b>26</b>	V
ICM Gain	$V_{CSSP-CSSN} = 110mV$		20		V/V
ICM Accuracy	$V_{CSSP-CSSN} = 110mV$	<b>-2.5</b>		<b>2.5</b>	%
	$V_{CSSP-CSSN} = 55mV$ or $35mV$	<b>-4</b>		<b>4</b>	%
	$V_{CSSP-CSSN} = 20mV$	<b>-8</b>		<b>8</b>	%
ICM Max Output Current	$V_{CSSP-CSSN} = 0.1V$			<b>500</b>	$\mu A$
<b>SUPPLY AND LINEAR REGULATOR</b>					
$DCIN$ , Input Voltage Range		<b>8</b>		<b>26</b>	V
VDDP Output Voltage	$8.0V < V_{DCIN} < 28V$ , no load	<b>4.9</b>	5.1	<b>5.3</b>	V
VDDP Load Regulation	$0 < I_{VDDP} < 30mA$		35	<b>100</b>	mV
VDDSMB Range		<b>2.7</b>		<b>5.5</b>	V
VDDSMB UVLO Rising		<b>2.4</b>	2.5	<b>2.6</b>	V
VDDSMB UVLO Hysteresis		<b>40</b>	100	<b>150</b>	mV
VDDSMB Quiescent Current	$V_{DDP} = SCL = SDA = 5.5V$		20	<b>27</b>	$\mu A$
<b>V REFERENCE</b>					
VREF Output Voltage	$0 < I_{VREF} < 300\mu A$	<b>3.1</b>	3.2	<b>3.3</b>	V
<b>ACOK</b>					
ACOK Sink Current	$V_{ACOK} = 0.4V$ , $ACIN = 1.5V$	<b>2</b>	8		mA
ACOK Leakage Current	$V_{ACOK} = 5.5V$ , $ACIN = 3.7V$			<b>1</b>	$\mu A$
<b>ACIN</b>					
ACIN Rising Threshold		<b>3.1</b>	3.2	<b>3.3</b>	V
ACIN Threshold Hysteresis		<b>40</b>	60	<b>90</b>	mV
ACIN Input Bias Current		<b>-1</b>		<b>1</b>	$\mu A$
<b>SWITCHING REGULATOR</b>					
Frequency		<b>330</b>	400	<b>440</b>	kHz

**Electrical Specifications** DCIN = CSSP = CSSN = 18V, CSOP = CSON = 12V, VDDP = 5V, BOOT-PHASE = 5.0V, GND = PGND = 0V, CVDDP = 1μF, IVDDP = 0mA, TA = -10°C to +100°C. **Boldface limits apply over the operating temperature range, -10°C to +100°C. (Continued)**

PARAMETER	CONDITIONS	MIN (Note 6)	TYP	MAX (Note 6)	UNITS
BOOT Supply Current	UGATE High	<b>170</b>	290	<b>400</b>	μA
PHASE Input Bias Current	V <sub>DCON</sub> = 28V, V <sub>CSON</sub> = V <sub>PHASE</sub> = 20V		0	<b>2</b>	μA
UGATE ON-Resistance Low	I <sub>UGATE</sub> = -100mA		0.9	<b>1.6</b>	Ω
UGATE ON-Resistance High	I <sub>UGATE</sub> = 10mA		1.4	<b>2.5</b>	Ω
LGATE ON-Resistance High	I <sub>LGATE</sub> = +10mA		1.4	<b>2.5</b>	Ω
LGATE ON-Resistance Low	I <sub>LGATE</sub> = -100mA		0.9	<b>1.6</b>	Ω
Dead Time	Falling UGATE to rising LGATE or falling LGATE to rising UGATE	<b>35</b>	50	<b>80</b>	ns
<b>ERROR AMPLIFIERS</b>					
GMV Amplifier Transconductance		<b>200</b>	250	<b>300</b>	μA/V
GMI Amplifier Transconductance		<b>40</b>	50	<b>60</b>	μA/V
GMS Amplifier Transconductance		<b>40</b>	50	<b>60</b>	μA/V
GMI/GMS Saturation Current		<b>15</b>	21	<b>25</b>	μA
GMV Saturation Current		<b>10</b>	17	<b>30</b>	μA
ICOMP, VCOMP Clamp Voltage	0.25V < V <sub>ICOMP</sub> , V <sub>COMP</sub> < 3.5V	<b>200</b>	300	<b>400</b>	mV
<b>LOGIC LEVELS</b>					
SDA/SCL Input Low Voltage	V <sub>DDSMB</sub> = 2.7V to 5.5V			<b>0.8</b>	V
SDA/SCL Input High Voltage	V <sub>DDSMB</sub> = 2.7V to 5.5V	<b>2</b>			V
SDA/SCL Input Bias Current	V <sub>DDSMB</sub> = 2.7V to 5.5V	<b>-1</b>		<b>1</b>	μA
SDA, Output Sink Current	V <sub>SDA</sub> = 0.4V	<b>7</b>	15		mA

NOTE:

6. Parameters with MIN and/or MAX limits are 100% tested at +25°C, unless otherwise specified. Temperature limits established by characterization and are not production tested.

### SMBus Timing Specification V<sub>DDSMB</sub> = 2.7V TO 5.5V

PARAMETERS	SYMBOL	CONDITIONS	MIN	TYP	MAX	UNITS
SMBus Frequency	FSMB		<b>10</b>		<b>100</b>	kHz
Bus Free Time	TBUF		<b>4.7</b>			μs
Start Condition Hold Time from SCL	THD:STA		<b>4</b>			μs
Start Condition Setup Time from SCL	TSU:STA		<b>4.7</b>			μs
Stop Condition Setup Time from SCL	TSU:STO		<b>4</b>			μs
SDA Hold Time from SCL	THD:DAT		<b>300</b>			ns
SDA Setup Time from SCL	TSU:DAT		<b>250</b>			ns
SCL Low Timeout (Note 7)	T <sub>TIMEOUT</sub>		<b>22</b>	<b>25</b>	<b>30</b>	ms
SCL Low Period	T <sub>LOW</sub>		<b>4.7</b>			μs
SCL High Period	T <sub>HIGH</sub>		<b>4</b>			μs
Maximum Charging Period Without a SMBus Write to ChargeVoltage or ChargeCurrent Register			<b>140</b>	<b>180</b>	<b>220</b>	s

NOTES:

7. If SCL is low for longer than the specified time, the charger is disabled.

# Typical Operating Performance

DCIN = 20V, 3S2P Li-Battery,  $T_A = +25^\circ\text{C}$ , unless otherwise noted.

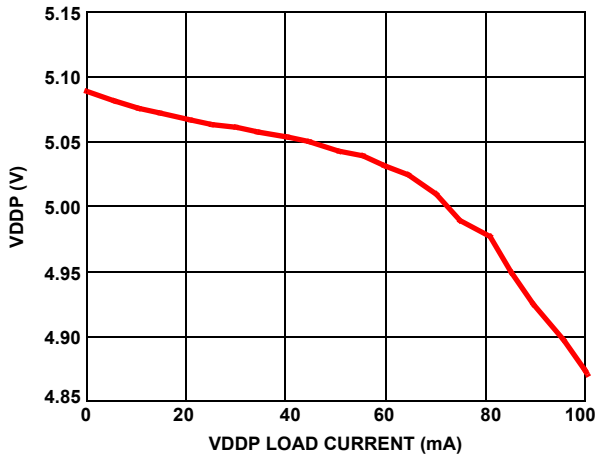


FIGURE 3. VDD LOAD REGULATION

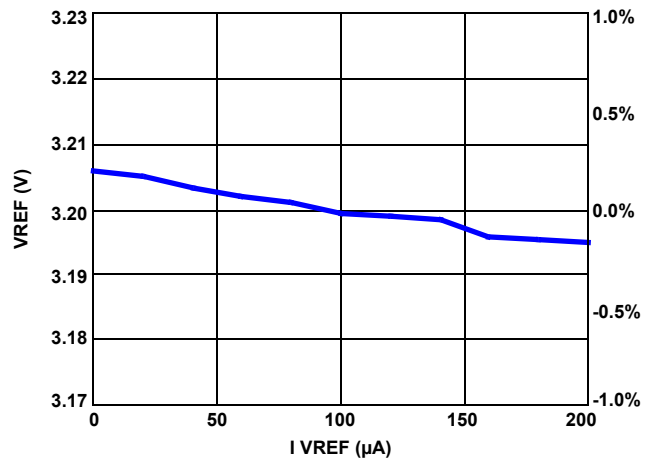


FIGURE 4. VREF LOAD REGULATION

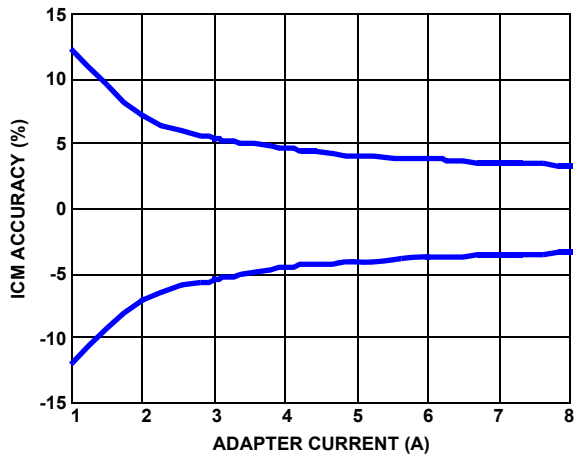


FIGURE 5. ICM ACCURACY vs AC-ADAPTER CURRENT

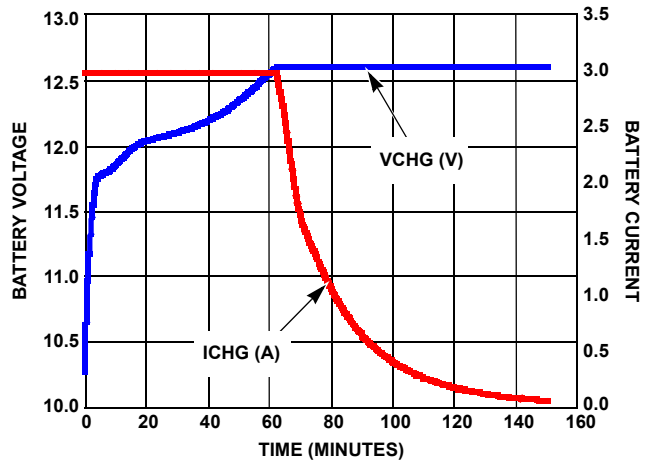


FIGURE 6. TYPICAL CHARGING VOLTAGE AND CURRENT

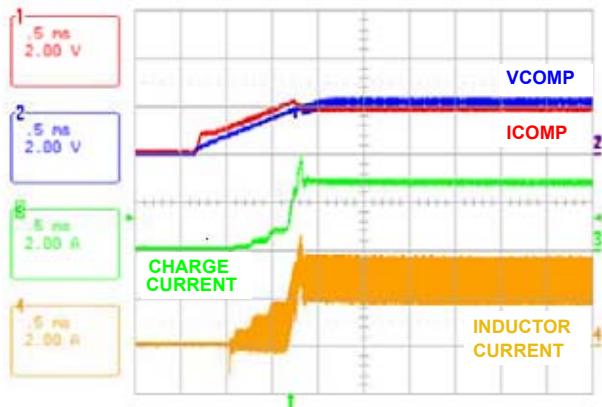


FIGURE 7. CHARGE ENABLE

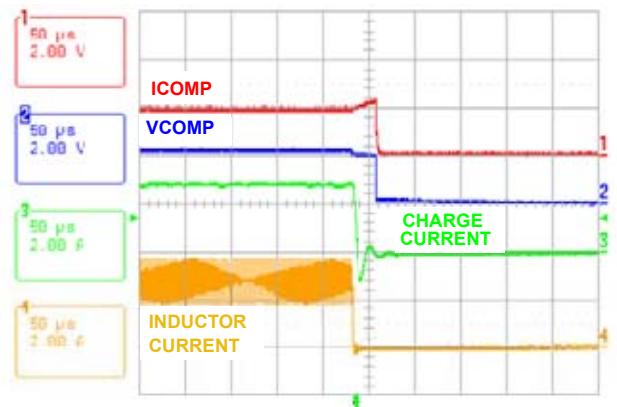


FIGURE 8. CHARGE DISABLE

# Typical Operating Performance

DCIN = 20V, 3S2P Li-Battery,  $T_A = +25^\circ\text{C}$ , unless otherwise noted.

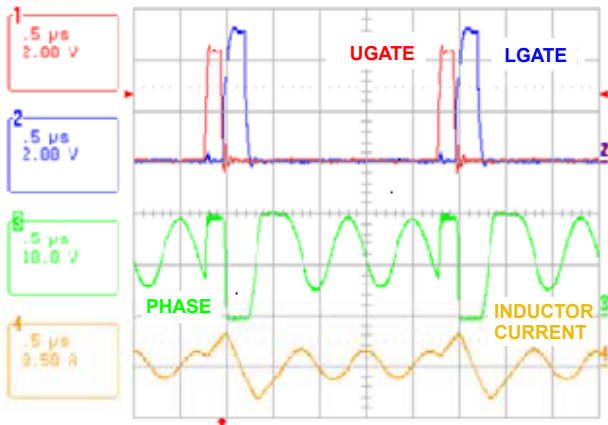


FIGURE 9. SWITCHING WAVEFORMS AT DIODE EMULATION

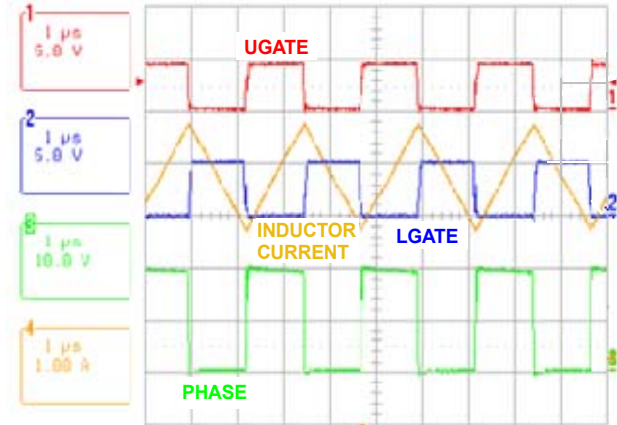


FIGURE 10. SWITCHING WAVEFORMS IN CC MODE

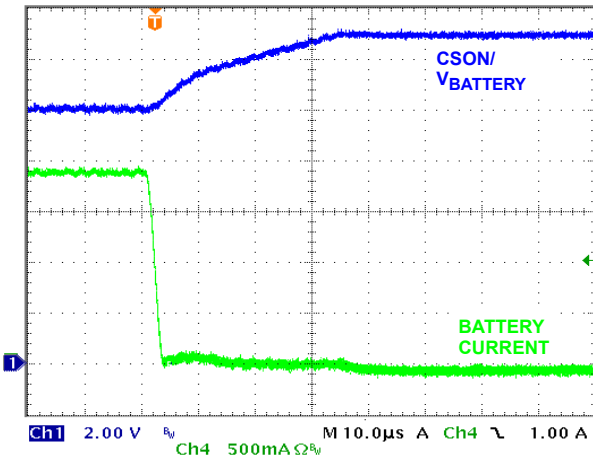


FIGURE 11. BATTERY REMOVAL

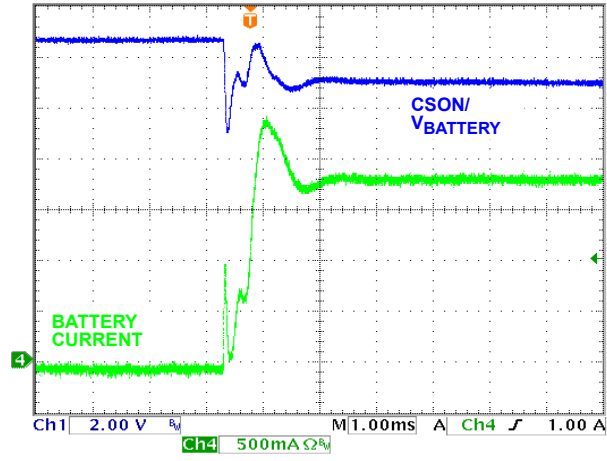


FIGURE 12. BATTERY INSERTION

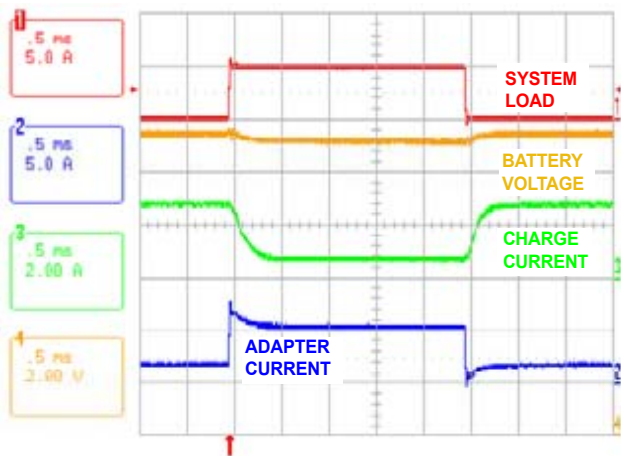


FIGURE 13. LOAD TRANSIENT RESPONSE

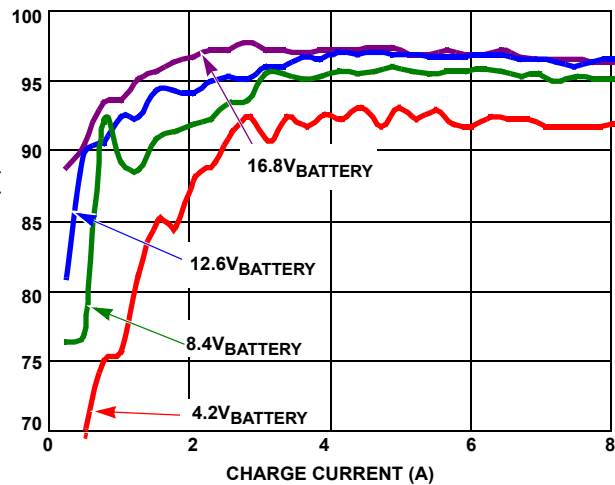


FIGURE 14. EFFICIENCY vs CHARGE CURRENT AND BATTERY VOLTAGE (EFFICIENCY DCIN = 20V)

## Functional Pin Descriptions

### BOOT

High-Side Power MOSFET Driver Power-Supply Connection. Connect a 0.1 $\mu$ F capacitor from BOOT to PHASE.

### UGATE

High-Side Power MOSFET Driver Output. Connect to the high-side N-Channel MOSFET gate.

### LGATE

Low-Side Power MOSFET Driver Output. Connect to low-side N-Channel MOSFET. LGATE drives between VDDP and PGND.

### PHASE

High-Side Power MOSFET Driver Source Connection. Connect to the source of the high-side N-Channel MOSFET.

### CSOP

Charge Current-Sense Positive Input.

### CSON

Charge Current-Sense Negative Input.

### CSSP

Input Current-Sense Positive Input.

### CSSN

Input Current-Sense Negative Input.

### DCIN

Charger Bias Supply Input. Bypass DCIN with a 0.1 $\mu$ F capacitor to GND.

### ACIN

AC-adaptor Detection Input. Connect to a resistor divider from the AC-adaptor output.

### ACOK

AC Detect Output. This open drain output is high impedance when ACIN is greater than 3.2V. The ACOK output remains low when the ISL88731A is powered down. Connect a 10k pull-up resistor from ACOK to VDDSMB.

### ICM

Input Current Monitor Output. ICM voltage equals  $20 \times (V_{CSSP} - V_{CSSN})$ .

### VREF

VREF is a reference output pin. It is internally compensated. Do not connect a decoupling capacitor.

### PGND

Power Ground. Connect PGND to the source of the low side MOSFET.

### VCC

Power input for internal analog circuits. Connect a 4.7 $\Omega$  resistor from VCC to VDDP and a 1 $\mu$ F ceramic capacitor from VCC to ground.

### VDDP

Linear Regulator Output. VDDP is the output of the 5.2V linear regulator supplied from DCIN. VDDP also directly supplies the LGATE driver and the BOOT strap diode. Bypass with a 1 $\mu$ F ceramic capacitor from VDDP to PGND.

### ICOMP

Compensation Point for the charging current and adapter current regulation Loop. Connect 0.01 $\mu$ F to GND. See "Voltage Control Loop" on page 20 for details of selecting the ICOMP capacitor.

### VCOMP

Compensation Point for the voltage regulation loop. Connect 4.7k $\Omega$  in series with 0.01 $\mu$ F to GND. See "Voltage Control Loop" on page 20 for details on selecting VCOMP components.

### VFB

Feedback for the Battery Voltage.

### VDDSMB

SMBus interface Supply Voltage Input. Bypass with a 0.1 $\mu$ F capacitor to GND.

### SDA

SMBus Data I/O. Open-drain Output. Connect an external pull-up resistor according to SMBus specifications.

### SCL

SMBus Clock Input. Connect an external pull-up resistor according to SMBus specifications.

### GND

Analog Ground. Connect directly to the backside paddle. Connect to PGND close to the output capacitor.

### Back Side Paddle

Connect the backside paddle to GND.

### NC

No Connect. Pins 1, 5, 7 and 14 are not connected.



## Theory of Operation

### Introduction

The ISL88731A includes all of the functions necessary to charge 1-to-4 cell Li-ion and Li-polymer batteries. A high efficiency synchronous buck converter is used to control the charging voltage up to 19.2V and charging current up to 8A. The ISL88731A also has input current limiting up to 11A. The Input current limit, charge current limit and charge voltage limit are set by internal registers written with SMBus. Figure 2 shows the ISL88731A “Typical Application Circuit”.

The ISL88731A charges the battery with constant charge current, set by the ChargeCurrent register, until the battery voltage rises to a voltage set by the ChargeVoltage register. The charger will then operate at a constant voltage. The adapter current is monitored and if the adapter current rises to the limit set by the InputCurrent register, battery charge current is reduced so the charger does not reduce the adapter current available to the system.

The ISL88731A features a voltage regulation loop (VCOMP) and two current regulation loops (ICOMP). The VCOMP voltage regulation loop monitors VFB to limit the battery charge voltage. The ICOMP current regulation loop limits the battery charging current delivered to the battery to ensure that it never exceeds the current set by the ChargeCurrent register. The ICOMP current regulation loop also limits the input current drawn from the AC-adapter to ensure that it never exceeds the limit set by the InputCurrent register, and to prevent a system crash and AC-adapter overload.

### PWM Control

The ISL88731A employs a fixed frequency PWM control architecture with a feed-forward function. The feed-forward function maintains a constant modulator gain of 11 to achieve fast line regulation as the input voltage changes.

The duty cycle of the buck regulator is controlled by the lower of the voltages on ICOMP and VCOMP. The voltage on ICOMP and VCOMP are inputs to a Lower Voltage Buffer (LVB) whose output is the lower of the two inputs. The output of the LVB is compared to an internal 400kHz ramp to produce the Pulse Width Modulated signal that controls the UGATE and LGATE drivers. An internal clamp holds the higher of the two voltages (0.3V) above the lower voltage. This speeds the transition from voltage loop control to current loop control or vice versa.

The ISL88731A can operate up to 99.6% duty cycle if the input voltage drops close to or below the battery charge voltage (drop out mode). The DC/DC converter has a timer to prevent the frequency from dropping into the audible frequency range.

To prevent boosting of the system bus voltage, the battery charger drives the lower FET in a way that prevents negative inductor current.

An adaptive gate drive scheme is used to control the dead time between two switches. The dead time control circuit monitors the LGATE output and prevents the upper side MOSFET from turning on until 20ns after LGATE falls below 1V  $V_{GS}$ , preventing cross-conduction and shoot-through. The same occurs for LGATE turn on. In order for the dead time circuit to work properly, there must be a low resistance, low inductance path from the LGATE

driver to MOSFET gate, and from the source of MOSFET to PGND. An internal Schottky diode between the VDDP pin and BOOT pin keeps the bootstrap capacitor charged.

### AC-Adapter Detection

Connect the AC-adapter voltage through a resistor divider to ACIN to detect when AC power is available, as shown in Figure 2. ACOK is an open-drain output and is active low when ACIN is less than  $V_{th,fall}$  and high when ACIN is above  $V_{th,rise}$ . The ACIN rising threshold is 3.2V (typ) with 57mV hysteresis.

### Current Measurement

Use ICM to monitor the adapter current being sensed across CSSP and CSSN. The output voltage range is 0V to 2.5V. The voltage of ICM is proportional to the voltage drop across CSSP and CSSN, and is given by Equation 1:

$$ICM = 20 \cdot I_{INPUT} \cdot R_{S1} \quad (EQ. 1)$$

where  $I_{ADAPTER}$  is the DC current drawn from the AC-adapter. It is recommended to have an RC filter at the ICM output for minimizing the switching noise.

### VDDP Regulator

VDDP provides a 5.2V supply voltage from the internal LDO regulator from DCIN and can deliver up to 30mA of continuous current. The MOSFET drivers are powered by VDDP. VDDP also supplies power to VCC through a low-pass filter as shown in the “Typical Application Circuit” (see Figure 2) on page 2. Bypass VDDP and VCC with a 1 $\mu$ F capacitor.

### VDDSMB Supply

The VDDSMB input provides power to the SMBus interface. Connect VDDSMB to VCC, or apply an external supply to VDDSMB. Bypass VDDSMB to GND with a 0.1 $\mu$ F or greater ceramic capacitor.

The typical application connects VDDSMB to the same power source as the SMBus master. This supply should be active and greater than 2.5V when either the adapter or the battery is present.

ISL88731A does not function when VDDSMB is below its specified Under Voltage Lockout (UVLO) voltage. All of the SMBus registers in ISL88731A are powered by VDDSMB and are set to zero when it is below the UVLO threshold. Other functions are unpredictable when VDDSMB is below the UVLO threshold.

### Short Circuit Protection and 0V Battery Charging

Since the battery charger will regulate the charge current to the limit set by the ChargeCurrent register, it automatically has short circuit protection and is able to provide the charge current to wake up an extremely discharged battery. Undervoltage trickle charge folds back current if there is a short circuit on the output.

### Undervoltage Detect and Battery Trickle Charging

If the voltage at CSON falls below 2.5V, the ISL88731A reduces the charge current limit to 128mA to trickle charge the battery. When the voltage rises above 2.7V the charge current reverts to the programmed value in the ChargeCurrent register.

### Over-Temperature Protection

If the die temperature exceeds +150°C, it stops charging. Once the die temperature drops below +125°C, charging will start up again.

### Overvoltage Protection

ISL88731A has an Overvoltage Protection circuit that limits the output voltage when the battery is removed or disconnected by a pulse charging circuit. If CSON exceeds the output voltage set point in the charge voltage register by more than 300mV an internal comparator pulls VCOMP down and turns off both upper and lower FETs of the buck as in Figure 15. There is a delay of approximately 1µs between V<sub>OUT</sub> exceeding the OVP trip point and pulling VCOMP, LGATE and UGATE low. After UGATE and LGATE are turned OFF inductor current continues to flow through the body diode of the lower FET and V<sub>OUT</sub> continues to rise until inductor current reaches zero.

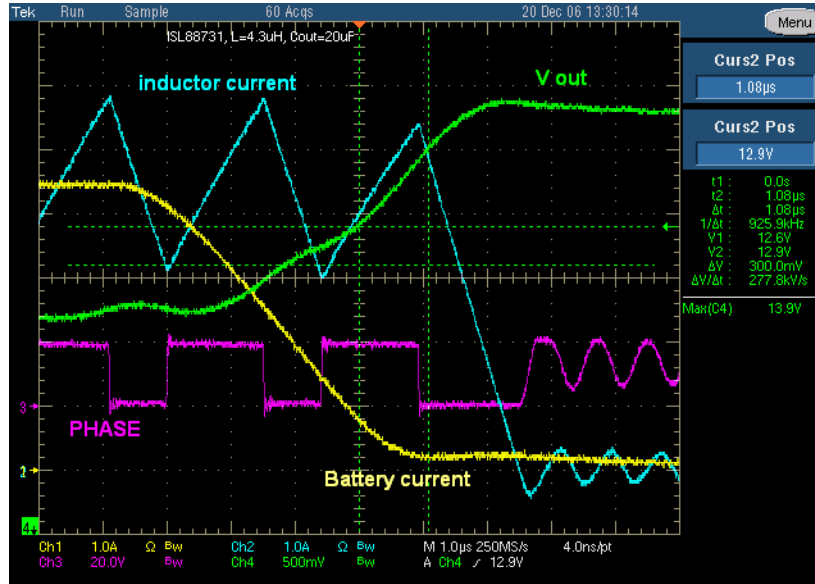
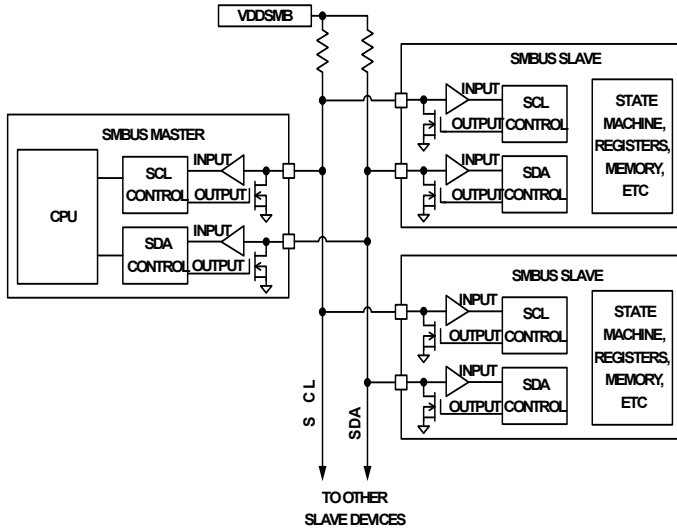


FIGURE 15. OVERVOLTAGE PROTECTION IN ISL88731A

## The System Management Bus

The System Management Bus (SMBus) is a 2-wire bus that supports bidirectional communications. The protocol is described briefly here. More detail is available from [www.smbus.org](http://www.smbus.org).

### General SMBus Architecture



### Data Validity

The data on the SDA line must be stable during the HIGH period of the SCL, unless generating a START or STOP condition. The HIGH or LOW state of the data line can only change when the clock signal on the SCL line is LOW. Refer to Figure 16.

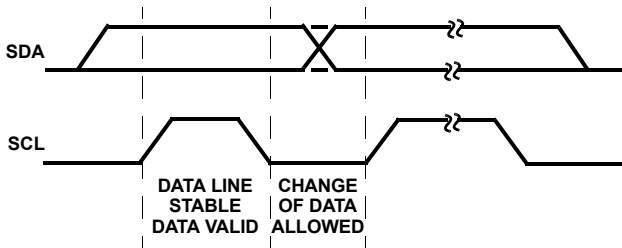


FIGURE 16. DATA VALIDITY

### START and STOP Conditions

As shown in Figure 17, START condition is a HIGH-to-LOW transition of the SDA line while SCL is HIGH.

The STOP condition is a LOW-to-HIGH transition on the SDA line while SCL is HIGH. A STOP condition must be sent before each START condition.

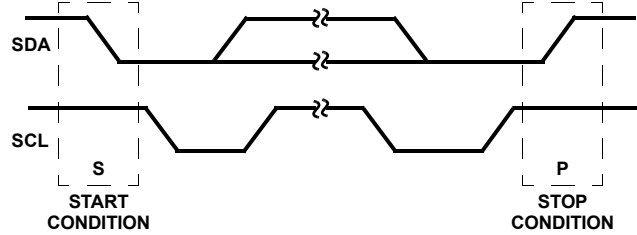


FIGURE 17. START AND STOP WAVEFORMS

### Acknowledge

Each address and data transmission uses 9-clock pulses. The ninth pulse is the acknowledge bit (ACK). After the start condition, the master sends 7-slave address bits and a R/W bit during the next 8-clock pulses. During the ninth clock pulse, the device that recognizes its own address holds the data line low to acknowledge. The acknowledge bit is also used by both the master and the slave to acknowledge receipt of register addresses and data (see Figure 18).

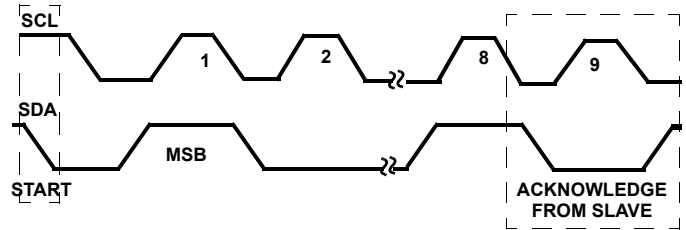


FIGURE 18. ACKNOWLEDGE ON THE I<sup>2</sup>C BUS

### SMBus Transactions

All transactions start with a control byte sent from the SMBus master device. The control byte begins with a Start condition, followed by 7-bits of slave address (0001001 for the ISL88731A) followed by the R/W bit. The R/W bit is 0 for a write or 1 for a read. If any slave devices on the SMBus bus recognize their address, they will Acknowledge by pulling the serial data (SDA) line low for the last clock cycle in the control byte. If no slaves exist at that address or are not ready to communicate, the data line will be 1, indicating a Not Acknowledge condition.

Once the control byte is sent, and the ISL88731A acknowledges it, the 2nd byte sent by the master must be a register address byte such as 0x14 for the ChargeCurrent register. The register address byte tells the ISL88731A which register the master will write or read. See Table 1 for details of the registers. Once the ISL88731A receives a register address byte it responds with an acknowledge.

**Write To A Register**



**Read From A Register**

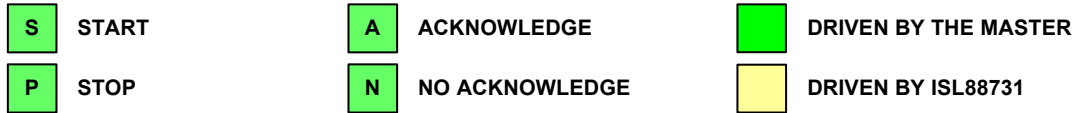
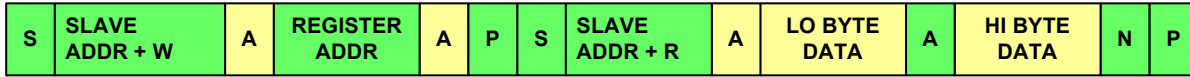


FIGURE 19. SMBus/ISL88731A READ AND WRITE PROTOCOL

**Byte Format**

Every byte put on the SDA line must be eight bits long and must be followed by an acknowledge bit. Data is transferred with the most significant bit first (MSB) and the least significant bit last (LSB).

The data (SDA) and clock (SCL) pins have Schmitt-trigger inputs that can accommodate slow edges. Choose pull-up resistors for SDA and SCL to achieve rise times according to the SMBus specifications. The ISL88731A is controlled by the data written to the registers described in Table 1.

**ISL88731A and SMBus**

The ISL88731A receives control inputs from the SMBus interface. The serial interface complies with the SMBus protocols as documented in the System Management Bus Specification V1.1, which can be downloaded from [www.smbus.org](http://www.smbus.org). The ISL88731A uses the SMBus Read-Word and Write-Word protocols (Figure 19) to communicate with the smart battery. The ISL88731A is an SMBus slave device and does not initiate communication on the bus. It responds to the 7-bit address 0b0001001\_ (0x12).

**Battery Charger Registers**

The ISL88731A supports five battery-charger registers that use either Write-Word or Read-Word protocols, as summarized in Table 1. ManufacturerID and DeviceID are “read only” registers and can be used to identify the ISL88731A. On the ISL88731A, ManufacturerID always returns 0x0049 (ASCII code for “I” for Intersil) and DeviceID always returns 0x0001.

Read address = 0b00010011 and

Write address = 0b00010010.

**Enabling and Disabling Charging**

After applying power to ISL88731A, the internal registers contain their POR values (see Table 1). The POR values for charge current and charge voltage are 0x0000. These values disable charging. To enable charging, the ChargeCurrent register must be written with a number >0x007F and the ChargeVoltage register must be written with a number >0x000F. Charging can be disabled by writing 0x0000 to either of these registers.

In addition, the ISL88731A has two identification (ID) registers: a 16-bit device ID register and a 16-bit manufacturer ID register.

TABLE 1. BATTERY CHARGER REGISTER SUMMARY

REGISTER ADDRESS	REGISTER NAME	READ/WRITE	DESCRIPTION	POR STATE
0x14	ChargeCurrent	Read or Write	6-bit Charge Current Setting	0x0000
0x15	ChargeVoltage	Read or Write	11-bit Charge Voltage Setting	0x0000
0x3F	InputCurrent	Read or Write	6-bit Charge Current Setting	0x0080
0xFE	ManufacturerID	Read Only	Manufacturer ID	0x0049
0xFF	DeviceID	Read Only	Device ID	0x0001

## Setting Charge Voltage

Charge voltage is set by writing a valid 16-bit number to the ChargeVoltage register. This 16-bit number translates to a 65.535V full-scale voltage. The ISL88731A ignores the first 4 LSBs and uses the next 11 bits to set the voltage DAC. The charge voltage range of the ISL88731A is 1.024V to 19.200V. Numbers requesting charge voltage greater than 19.200V result in a ChargeVoltage of 19.200V. All numbers requesting charge voltage below 1.024V result in a voltage set point of zero, which terminates charging. Upon initial power-up or reset, the ChargeVoltage and ChargeCurrent registers are reset to 0 and the charger remains shut down until valid numbers are sent to

the ChargeVoltage and ChargeCurrent registers. Use the Write-Word protocol (Figure 19) to write to the ChargeVoltage register. The register address for ChargeVoltage is 0x15. The 16-bit binary number formed by D15–D0 represents the charge voltage set point in mV. However, the resolution of the ISL88731A is 16mV because the D0–D3 bits are ignored as shown in Table 2. The D-5 bit is also ignored because it is not needed to span the 1.024V to 19.2V range. Table 2 shows the mapping between the charge-voltage set point and the 16-bit number written to the ChargeVoltage register. The ChargeVoltage register can be read back to verify its contents.

**TABLE 2. CHARGEVOLTAGE (REGISTER 0x15)**

BIT	BIT NAME	DESCRIPTION
0		Not used
1		Not used
2		Not used
3		Not used
4	Charge Voltage, DACV 0	0 = Adds 0mV of charger voltage, 1024mV min 1 = Adds 16mV of charger voltage
5	Charge Voltage, DACV 1	0 = Adds 0mV of charger voltage, 1024mV min 1 = Adds 32mV of charger voltage
6	Charge Voltage, DACV 2	0 = Adds 0mV of charger voltage, 1024mV min 1 = Adds 64mV of charger voltage
7	Charge Voltage, DACV 3	0 = Adds 0mV of charger voltage, 1024mV min 1 = Adds 128mV of charger voltage
8	Charge Voltage, DACV 4	0 = Adds 0mV of charger voltage, 1024mV min 1 = Adds 256mV of charger voltage
9	Charge Voltage, DACV 5	0 = Adds 0mV of charger voltage, 1024mV min 1 = Adds 512mV of charger voltage
10	Charge Voltage, DACV 6	0 = Adds 0mA of charger voltage 1 = Adds 1024mV of charger voltage
11	Charge Voltage, DACV 7	0 = Adds 0mV of charger voltage 1 = Adds 2048mV of charger voltage
12	Charge Voltage, DACV 8	0 = Adds 0mV of charger voltage 1 = Adds 4096mV of charger voltage
13	Charge Voltage, DACV 9	0 = Adds 0mV of charger voltage 1 = Adds 8192mV of charger voltage
14	Charge Voltage, DACV 10	0 = Adds 0mV of charger voltage 1 = Adds 16384mV of charger voltage, 19200mV max
15		Not used. Normally a 32768mV weight

## Setting Charge Current

ISL88731A has a 16-bit ChargeCurrent register that sets the battery charging current. ISL88731A controls the charge current by controlling the CSOP-CSON voltage. The register's LSB translates to 10 $\mu$ V at CSON-CSOP. With a 10m $\Omega$  charge current R<sub>sense</sub> resistor (RS2 in Figure 2), the LSB translates to 1mA charge current. The ISL88731A ignores the first 7 LSBs and uses the next 6 bits to control the current DAC. The charge-current range of the ISL88731A is 0 to 8.064A (using a 10m $\Omega$  current-sense resistor). All numbers requesting charge current above 8.064A result in a current setting of 8.064A. All numbers requesting charge current between 0mA to 128mA result in a current setting of 0mA. The default charge current setting at Power-On Reset (POR) is 0mA. To stop charging, set ChargeCurrent to 0. Upon initial power-up, the ChargeVoltage and ChargeCurrent registers are reset to 0 and the charger is

disabled. To start the charger, write valid numbers to the ChargeVoltage and ChargeCurrent registers. The ChargeCurrent register uses the Write-Word protocol (see Figure 19). The register code for ChargeCurrent is 0x14 (0b00010100). Table 3 shows the mapping between the charge current set point and the ChargeCurrent number. The ChargeCurrent register can be read back to verify its contents.

The ISL88731A includes a fault limiter for low battery conditions. If the battery voltage is less than 2.5V, the charge current is temporarily set to 128mA. The ChargeCurrent register is preserved and becomes active again when the battery voltage is higher than 2.7V. This function effectively provides a foldback current limit, which protects the charger during short circuit and overload.

**TABLE 3. CHARGE CURRENT (REGISTER 0x14) (10m $\Omega$  SENSE RESISTOR, RS2)**

BIT	BIT NAME	DESCRIPTION
0		Not used
1		Not used
2		Not used
3		Not used
4		Not used
5		Not used
6		Not used
7	Charge Current, DACI 0	0 = Adds 0mA of charger current 1 = Adds 128mA of charger current
8	Charge Current, DACI 1	0 = Adds 0mA of charger current 1 = Adds 256mA of charger current
9	Charge Current, DACI 2	0 = Adds 0mA of charger current 1 = Adds 512mA of charger current
10	Charge Current, DACI 3	0 = Adds 0mA of charger current 1 = Adds 1024mA of charger current
11	Charge Current, DACI 4	0 = Adds 0mA of charger current 1 = Adds 2048mA of charger current
12	Charge Current, DACI 5	0 = Adds 0mA of charger current 1 = Adds 4096mA of charger current, 8064mA max
13		Not used
14		Not used
15		Not used

## Setting Input-Current Limit

The total power from an AC-adaptor is the sum of the power supplied to the system and the power into the charger and battery. When the input current exceeds the set input current limit, the ISL88731A decreases the charge current to provide priority to system load current. As the system load rises, the available charge current drops linearly to zero. Thereafter, the total input current can increase to the limit of the AC-adaptor.

The internal amplifier compares the differential voltage between CSSP and CSSN to a scaled voltage set by the InputCurrent register. The total input current is the sum of the device supply current, the charger input current, and the system load current. The total input current can be estimated by using Equation 2.

$$I_{\text{INPUT}} = I_{\text{SYSTEM}} + [(I_{\text{CHARGE}} \times V_{\text{BATTERY}}) / (V_{\text{IN}} \times \eta)] \quad (\text{EQ. 2})$$

Where  $\eta$  is the efficiency of the DC/DC converter (typically 85% to 95%).

The ISL88731A has a 16-bit InputCurrent register that translates to a 2mA LSB and a 131.071A full-scale current using a 10m $\Omega$  current-sense resistor (RS1 in Figure 2). Equivalently, the 16-bit InputCurrent number sets the voltage across CSSP and CSSN

inputs in 20 $\mu$ V per LSB increments. To set the input current limit use the SMBus to write a 16-bit InputCurrent register using the data format listed in Table 4. The InputCurrent register uses the Write-Word protocol (see Figure 19). The register code for InputCurrent is 0x3F (0b00111111). The InputCurrent register can be read back to verify its contents.

The ISL88731A ignores the first 7 LSBs and uses the next 6 bits to control the input-current DAC. The input-current range of the ISL88731A is from 256mA to 11.004A. All 16-bit numbers requesting input current above 11.004A result in an input-current setting of 11.004A. All 16-bit numbers requesting input current between 0mA to 256mA result in an input-current setting of 0mA. The default input-current-limit setting at POR is 256mA. When choosing the current-sense resistor RS1, carefully calculate its power rating. Take into account variations in the system's load current and the overall accuracy of the sense amplifier. Note that the voltage drop across RS1 contributes additional power loss, which reduces efficiency. System currents normally fluctuate as portions of the system are powered up or put to sleep. Without input current regulation, the input source must be able to deliver the maximum system current and the maximum charger-input current. By using the input-current-limit circuit, the output-current capability of the AC wall adapter can be lowered, reducing system cost.

**TABLE 4. INPUT CURRENT (REGISTER 0x3F) (10m $\Omega$  SENSE RESISTOR, RS1)**

BIT	BIT NAME	DESCRIPTION
0		Not used
1		Not used
2		Not used
3		Not used
4		Not used
5		Not used
6		Not used
7	Input Current, DACS 0	0 = Adds 0mA of input current 1 = Adds 256mA of input current
8	Input Current, DACS 1	0 = Adds 0mA of input current 1 = Adds 512mA of input current
9	Input Current, DACS 2	0 = Adds 0mA of input current 1 = Adds 1024mA of input current
10	Input Current, DACS 3	0 = Adds 0mA of input current 1 = Adds 2048mA of input current
11	Input Current, DACS 4	0 = Adds 0mA of input current 1 = Adds 4096mA of input current
12	Input Current, DACS 5	0 = Adds 0mA of input current 1 = Adds 8192mA of input current, 11004mA max
13		Not used
14		Not used
15		Not used

## Charger Timeout

The ISL88731A includes 2 timers to insure the SMBus master is active and to prevent overcharging the battery. ISL88731A will terminate charging if the charger has not received a write to the ChargeVoltage or ChargeCurrent register within 175s or if the SCL line is low for more than 25ms. If a time-out occurs, either ChargeVoltage or ChargeCurrent registers must be written to re-enable charging.

## ISL88731A Data Byte Order

Each register in ISL88731A contains 16bits or 2, 8 bit bytes. All data sent on the SMBus is in 8-bit bytes and 2 bytes must be written or read from each register in ISL88731A. The order in which these bytes are transmitted appears reversed from the way they are normally written. The LOW byte is sent first and the HI byte is sent second. For example, When writing 0x41A0, 0xA0 is written first and 0x41 is sent second.

## Writing to the Internal Registers

In order to set the charge current, charge voltage or input current, valid 16-bit numbers must be written to ISL88731A's internal registers via the SMBus.

To write to a register in the ISL88731A, the master sends a control byte with the  $R/\bar{W}$  bit set to 0, indicating a write. If it receives an Acknowledge from the ISL88731A it sends a register address byte setting the register to be written (i.e. 0x14 for the ChargeCurrent register). The ISL88731A will respond with an Acknowledge. The master then sends the lower data byte to be written into the desired register. The ISL88731A will respond with an Acknowledge. The master then sends the higher data byte to be written into the desired register. The ISL88731A will respond with an Acknowledge. The master then issues a Stop condition, indicating to the ISL88731A that the current transaction is complete. Once this transaction completes, the ISL88731A will begin operating at the new current or voltage.

ISL88731A does not support writing more than one register per transaction.

## Reading from the Internal Registers

The ISL88731A has the ability to read from 5 internal registers. Prior to reading from an internal register, the master must first select the desired register by writing to it and sending the registers address byte. This process begins by the master sending a control byte with the  $R/\bar{W}$  bit set to 0, indicating a write. Once it receives an Acknowledge from the ISL88731A it sends a register address byte representing the internal register it wants to read. The ISL88731A will respond with an Acknowledge. The master must then respond with a Stop condition. After the Stop condition, the master follows with a new Start condition, then sends a new control byte with the ISL88731A slave address and the  $R/\bar{W}$  bit set to 1, indicating a read. The ISL88731A will Acknowledge then send the lower byte stored in that register. After receiving the byte, the master Acknowledges by holding SDA low during the 9th clock pulse. ISL88731A then sends the higher byte stored in the register. After the second byte, neither device holds SDA low (No

Acknowledge). The master will then produce a Stop condition to end the read transaction.

ISL88731A does not support reading more than 1 register per transaction.

## Application Information

The following battery charger design refers to the "Typical Application Circuit" (see Figure 2) on page 2, where typical battery configuration of 3S2P is used. This section describes how to select the external components including the inductor, input and output capacitors, switching MOSFETs and current sensing resistors.

### Inductor Selection

The inductor selection has trade-offs between cost, size, crossover frequency and efficiency. For example, the lower the inductance, the smaller the size, but ripple current is higher. This also results in higher AC losses in the magnetic core and the windings, which decreases the system efficiency. On the other hand, the higher inductance results in lower ripple current and smaller output filter capacitors, but it has higher DCR (DC resistance of the inductor) loss, lower saturation current and has slower transient response. So, the practical inductor design is based on the inductor ripple current being  $\pm 15\%$  to  $\pm 20\%$  of the maximum operating DC current at maximum input voltage. Maximum ripple is at 50% duty cycle or  $V_{BAT} = V_{IN,MAX}/2$ . The required inductance for  $\pm 15\%$  ripple current can be calculated from Equation 3:

$$L = \frac{V_{IN,MAX}}{4 \cdot F_{SW} \cdot 0.3 \cdot I_{L,MAX}} \quad (\text{EQ. 3})$$

Where,  $V_{IN,(MAX)}$  is the maximum input voltage,  $F_{SW}$  is the switching frequency and  $I_{L,(MAX)}$  is the max DC current in the inductor.

For  $V_{IN,(MAX)} = 20V$ ,  $V_{BAT} = 12.6V$ ,  $I_{BAT,(MAX)} = 4.5A$ , and  $f_s = 400kHz$ , the calculated inductance is  $9.3\mu H$ . Choosing the closest standard value gives  $L = 10\mu H$ . Ferrite cores are often the best choice since they are optimized at 400kHz to 600kHz operation with low core loss. The core must be large enough not to saturate at the peak inductor current  $I_{PEAK}$  in Equation 4:

$$I_{PEAK} = I_{L,MAX} + \frac{1}{2} \cdot I_{RIPPLE} \quad (\text{EQ. 4})$$

Inductor saturation can lead to cascade failures due to very high currents. Conservative design limits the peak and RMS current in the inductor to less than 90% of the rated saturation current.

Crossover frequency is heavily dependent on the inductor value.  $F_{CO}$  should be less than 20% of the switching frequency and a conservative design has  $F_{CO}$  less than 10% of the switching frequency. The highest  $F_{CO}$  is in voltage control mode with the battery removed and may be calculated (approximately) from Equation 5:

$$F_{CO} = \frac{5 \cdot 11 \cdot R_{SENSE}}{2\pi \cdot L} \quad (\text{EQ. 5})$$



## Output Capacitor Selection

The output capacitor in parallel with the battery is used to absorb the high frequency switching ripple current and smooth the output voltage. The RMS value of the output ripple current  $I_{RMS}$  is given by Equation 6:

$$I_{RMS} = \frac{V_{IN,MAX}}{\sqrt{12} \cdot L \cdot F_{SW}} \cdot D \cdot (1 - D) \quad (\text{EQ. 6})$$

Where the duty cycle  $D$  is the ratio of the output voltage (battery voltage) over the input voltage for continuous conduction mode which is typical operation for the battery charger. During the battery charge period, the output voltage varies from its initial battery voltage to the rated battery voltage. So, the duty cycle varies from 0.53 for the minimum battery voltage of 7.5V (2.5V/Cell) to 0.88 for the maximum battery voltage of 12.6V. The maximum RMS value of the output ripple current occurs at the duty cycle of 0.5 and is expressed as Equation 7:

$$I_{RMS} = \frac{V_{IN,MAX}}{4 \cdot \sqrt{12} \cdot L \cdot F_{SW}} \quad (\text{EQ. 7})$$

For  $V_{IN,(MAX)} = 19V$ ,  $V_{BAT} = 16.8V$ ,  $L = 10\mu H$ , and  $f_s = 400kHz$ , the maximum RMS current is 0.19A. A typical 20 $\mu F$  ceramic capacitor is a good choice to absorb this current and also has very small size. Organic polymer capacitors have high capacitance with small size and have a significant equivalent series resistance (ESR). Although ESR adds to ripple voltage, it also creates a high frequency zero that helps the closed loop operation of the buck regulator.

EMI considerations usually make it desirable to minimize ripple current in the battery leads. Beads may be added in series with the battery pack to increase the battery impedance at 400kHz switching frequency. Switching ripple current splits between the battery and the output capacitor depending on the ESR of the output capacitor and battery impedance. If the ESR of the output capacitor is 10m $\Omega$  and battery impedance is raised to 2 $\Omega$  with a bead, then only 0.5% of the ripple current will flow in the battery.

## MOSFET Selection

The Notebook battery charger synchronous buck converter has the input voltage from the AC-adaptor output. The maximum AC-adaptor output voltage does not exceed 25V. Therefore, 30V logic MOSFET should be used.

The high-side MOSFET must be able to dissipate the conduction losses plus the switching losses. For the battery charger application, the input voltage of the synchronous buck converter is equal to the AC-adaptor output voltage, which is relatively constant. The maximum efficiency is achieved by selecting a high-side MOSFET that has the conduction losses equal to the switching losses. Switching losses in the low-side FET are very small. The choice of low-side FET is a trade-off between conduction losses ( $r_{DS(ON)}$ ) and cost. A good rule of thumb for the  $r_{DS(ON)}$  of the low-side FET is 2x the  $r_{DS(ON)}$  of the high-side FET.

The LGATE gate driver can drive sufficient gate current to switch most MOSFETs efficiently. However, some FETs may exhibit cross conduction (or shoot-through) due to current injected into the drain-to-source parasitic capacitor ( $C_{gd}$ ) by the high  $dV/dt$  rising edge at the phase node when the high-side MOSFET turns on.

Although LGATE sink current (1.8A typical) is more than enough to switch the FET off quickly, voltage drops across parasitic impedances between LGATE and the MOSFET can allow the gate to rise during the fast rising edge of voltage on the drain. MOSFETs with low threshold voltage (<1.5V) and low ratio of  $C_{gs}/C_{gd}$  (<5) and high gate resistance (>4 $\Omega$ ) may be turned on for a few ns by the high  $dV/dt$  (rising edge) on their drain. This can be avoided with higher threshold voltage and  $C_{gs}/C_{gd}$  ratio. Another way to avoid cross conduction is slowing the turn-on speed of the high-side MOSFET by connecting a resistor between the BOOT pin and the boot strap capacitor.

For the high-side MOSFET, the worst-case conduction losses occur at the minimum input voltage, as shown in Equation 8:

$$P_{Q1,conduction} = \frac{V_{OUT}}{V_{IN}} \cdot I_{BAT}^2 \cdot r_{DS(ON)} \quad (\text{EQ. 8})$$

The optimum efficiency occurs when the switching losses equal the conduction losses. However, it is difficult to calculate the switching losses in the high-side MOSFET since it must allow for difficult-to-quantify factors that influence the turn-on and turn-off times. These factors include the MOSFET internal gate resistance, gate charge, threshold voltage, stray inductance and the pull-up and pull-down resistance of the gate driver.

The following switching loss calculation (Equation 9) provides a rough estimate.

$$P_{Q1,Switching} = \frac{1}{2} V_{IN} I_{LV} f_{sw} \left( \frac{Q_{gd}}{I_{g,source}} \right) + \frac{1}{2} V_{IN} I_{LP} f_{sw} \left( \frac{Q_{gd}}{I_{g,sink}} \right) + Q_{rr} V_{IN} f_{sw} \quad (\text{EQ. 9})$$

Where, the following are the peak gate-drive source/sink current of  $Q_1$ , respectively:

- $Q_{gd}$ : drain-to-gate charge,
- $Q_{rr}$ : total reverse recovery charge of the body-diode in low-side MOSFET,
- $I_{LV}$ : inductor valley current,
- $I_{LP}$ : Inductor peak current,
- $I_{g,sink}$
- $I_{g,source}$

Low switching loss requires low drain-to-gate charge  $Q_{gd}$ . Generally, the lower the drain-to-gate charge, the higher the ON-resistance. Therefore, there is a trade-off between the ON-resistance and drain-to-gate charge. Good MOSFET selection is based on the Figure of Merit (FOM), which is a product of the total gate charge and ON-resistance. Usually, the smaller the value of FOM, the higher the efficiency for the same application.

For the low-side MOSFET, the worst-case power dissipation occurs at minimum battery voltage and maximum input voltage (Equation 10):

$$P_{Q2} = \left( 1 - \frac{V_{OUT}}{V_{IN}} \right) \cdot I_{BAT}^2 \cdot r_{DS(ON)} \quad (\text{EQ. 10})$$

Choose a low-side MOSFET that has the lowest possible ON-resistance with a moderate-sized package like the SO-8 and is reasonably priced. The switching losses are not an issue for the low-side MOSFET because it operates at zero-voltage-switching.

Ensure that the required total gate drive current for the selected MOSFETs should be less than 24mA. So, the total gate charge for the high-side and low-side MOSFETs is limited by Equation 11:

$$Q_{\text{GATE}} \leq \frac{I_{\text{GATE}}}{f_{\text{sw}}} \quad (\text{EQ. 11})$$

Where  $I_{\text{GATE}}$  is the total gate drive current and should be less than 24mA. Substituting  $I_{\text{GATE}} = 24\text{mA}$  and  $f_s = 400\text{kHz}$  into Equation 11 yields that the total gate charge should be less than 80nC. Therefore, the ISL88731A easily drives the battery charge current up to 8A.

## Snubber Design

ISL88731A's buck regulator operates in discontinuous current mode (DCM) when the load current is less than half the peak-to-peak current in the inductor. After the low-side FET turns off, the phase voltage rings due to the high impedance with both FETs off. This can be seen in Figure 9. Adding a snubber (resistor in series with a capacitor) from the phase node to ground can greatly reduce the ringing. In some situations a snubber can improve output ripple and regulation.

The snubber capacitor should be approximately twice the parasitic capacitance on the phase node. This can be estimated by operating at very low load current (100mA) and measuring the ringing frequency.

$C_{\text{SNUB}}$  and  $R_{\text{SNUB}}$  can be calculated from Equations 12 and 13:

$$C_{\text{SNUB}} = \frac{2}{(2\pi f_{\text{ring}})^2 \cdot L} \quad R_{\text{SNUB}} = \sqrt{\frac{2 \cdot L}{C_{\text{SNUB}}}} \quad (\text{EQ. 12}) \quad (\text{EQ. 13})$$

## Input Capacitor Selection

The input capacitor absorbs the ripple current from the synchronous buck converter, which is given by Equation 14:

$$I_{\text{rms}} = I_{\text{BAT}} \frac{\sqrt{V_{\text{OUT}}(V_{\text{IN}} - V_{\text{OUT}})}}{V_{\text{IN}}} \quad (\text{EQ. 14})$$

This RMS ripple current must be smaller than the rated RMS current in the capacitor datasheet. Non-tantalum chemistries (ceramic, aluminum, or OSCON) are preferred due to their resistance to power-up surge currents when the AC-adaptor is plugged into the battery charger. For Notebook battery charger applications, it is recommended that ceramic capacitors or polymer capacitors from Sanyo be used due to their small size and reasonable cost.

## Loop Compensation Design

ISL88731A has three closed loop control modes. One controls the output voltage when the battery is fully charged or absent. A second controls the current into the battery when charging and the third limits current drawn from the adapter. The charge current and input current control loops are compensated by a single capacitor on the ICOMP pin. The voltage control loop is compensated by a network on the VCOMP pin. Descriptions of these control loops and guidelines for selecting compensation components will be given in the following sections. Which loop controls the output is determined by the minimum current buffer and the minimum voltage buffer shown in the "Functional Block

Diagram" (see Figure 1) on page 2. These three loops will be described separately.

## Transconductance Amplifiers GMV, GMI and GMS

ISL88731A uses several transconductance amplifiers (also known as gm amps). Most commercially available op amps are voltage controlled voltage sources with gain expressed as  $A = V_{\text{OUT}}/V_{\text{IN}}$ . gm amps are voltage controlled current sources with gain expressed as  $gm = I_{\text{OUT}}/V_{\text{IN}}$ . gm will appear in some of the equations for poles and zeros in the compensation.

## PWM Gain $F_m$

The Pulse Width Modulator in the ISL88731A converts voltage at VCOMP to a duty cycle by comparing VCOMP to a triangle wave (duty =  $V_{\text{COMP}}/V_{\text{P-P RAMP}}$ ). The low-pass filter formed by L and  $C_o$  convert the duty cycle to a DC output voltage ( $V_o = V_{\text{DCIN}} \cdot \text{duty}$ ). In ISL88731A, the triangle wave amplitude is proportional to  $V_{\text{DCIN}}$ . Making the ramp amplitude proportional to  $V_{\text{DCIN}}$  makes the gain from VCOMP to the PHASE output a constant 11 and is independent of  $V_{\text{DCIN}}$ . For small signal AC analysis, the battery is modeled by its internal resistance. The total output resistance is the sum of the sense resistor and the internal resistance of the MOSFETs, inductor and capacitor. Figure 20 shows the small signal model of the pulse width modulator (PWM), power stage, output filter and battery.

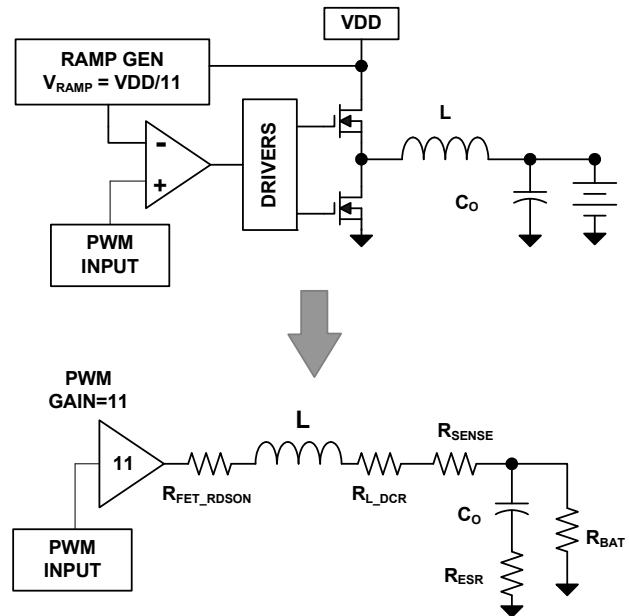


FIGURE 20. SMALL SIGNAL AC MODEL

In most cases the Battery resistance is very small (<200mΩ) resulting in a very low Q in the output filter. This results in a frequency response from the input of the PWM to the inductor current with a single pole at the frequency calculated in Equation 15:

$$F_{\text{POLE1}} = \frac{(R_{\text{SENSE}} + r_{\text{DS(ON)}} + R_{\text{DCR}} + R_{\text{BAT}})}{2\pi \cdot L} \quad (\text{EQ. 15})$$

The output capacitor creates a pole at a very high frequency due to the small resistance in parallel with it. The frequency of this pole is calculated in Equation 16:

$$F_{POLE2} = \frac{1}{2\pi \cdot C_o \cdot R_{BAT}} \quad (EQ. 16)$$

### Charge Current Control Loop

When the battery is less than the fully charged, the voltage error amplifier goes to it's maximum output (limited to 0.3V above ICOMP) and the ICOMP voltage controls the loop through the minimum voltage buffer. Figure 22 shows the charge current control loop.

The compensation capacitor ( $C_{ICOMP}$ ) gives the error amplifier (GMI) a pole at a very low frequency ( $\ll 1\text{Hz}$ ) and a zero at  $F_{Z1}$ .  $F_{Z1}$  is created by the  $0.25 \cdot CA2$  output added to ICOMP. The frequency can be calculated from Equation 17:

$$F_{ZERO} = \frac{4 \cdot gm2}{(2\pi \cdot C_{ICOMP})} \quad gm2 = 50\mu\text{A/V} \quad (EQ. 17)$$

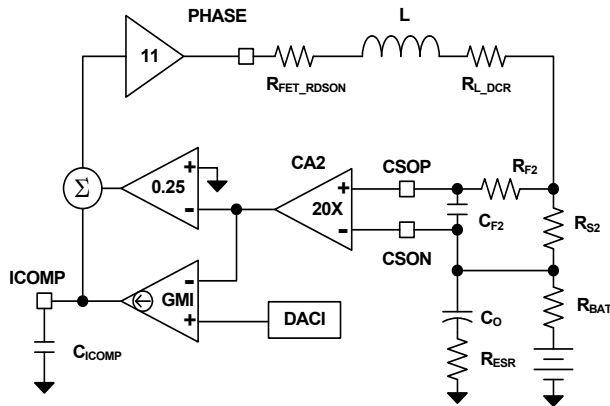


FIGURE 21. CHARGE CURRENT LIMIT LOOP

Placing this zero at a frequency equal to the pole calculated in Equation 16 will result in maximum gain at low frequencies and phase margin near  $90^\circ$ . If the zero is at a higher frequency (smaller  $C_{ICOMP}$ ), the DC gain will be higher but the phase margin will be lower. Use a capacitor on ICOMP that is equal to or greater than the value calculated in Equation 18. The factor of 1.5 is to ensure the zero is at a frequency lower than the pole including tolerance variations.

$$C_{ICOMP} = \frac{1.5 \cdot 4 \cdot (50\mu\text{A/V}) \cdot L}{(R_{SENSE} + r_{DS(ON)} + R_{DCR} + R_{BAT})} \quad (EQ. 18)$$

A filter should be added between  $R_{S2}$  and CSOP and CSON to reduce switching noise. The filter roll-off frequency should be between the crossover frequency and the switching frequency ( $\sim 100\text{kHz}$ ).  $R_{F2}$  should be small ( $< 10\Omega$ ) to minimize offsets due to leakage current into CSOP. The filter cut off frequency is calculated using Equation 19:

$$F_{FILTER} = \frac{1}{(2\pi \cdot C_{F2} \cdot R_{F2})} \quad (EQ. 19)$$

The crossover frequency is determined by the DC gain of the modulator and output filter and the pole in Equation 16. The DC gain is calculated in Equation 20 and the crossover frequency is calculated with Equation 21:

$$A_{DC} = \frac{11 \cdot R_{SENSE}}{(R_{SENSE} + r_{DS(ON)} + R_{DCR} + R_{BAT})} \quad (EQ. 20)$$

$$F_{CO} = A_{DC} \cdot F_{POLE} = \frac{11 \cdot R_{SENSE}}{2\pi \cdot L} \quad (EQ. 21)$$

The Bode plot of the loop gain, the compensator gain and the power stage gain is shown in Figure 22.

### Adapter Current Limit Control Loop

If the combined battery charge current and system load current draws current that equals the adapter current limit set by the InputCurrent register, ISL88731A will reduce the current to the battery and/or reduce the output voltage to hold the adapter current at the limit. Above the adapter current limit, the minimum current buffer equals the output of GMS and ICOMP controls the charger output. Figure 23 shows the adapter current limit control loop.

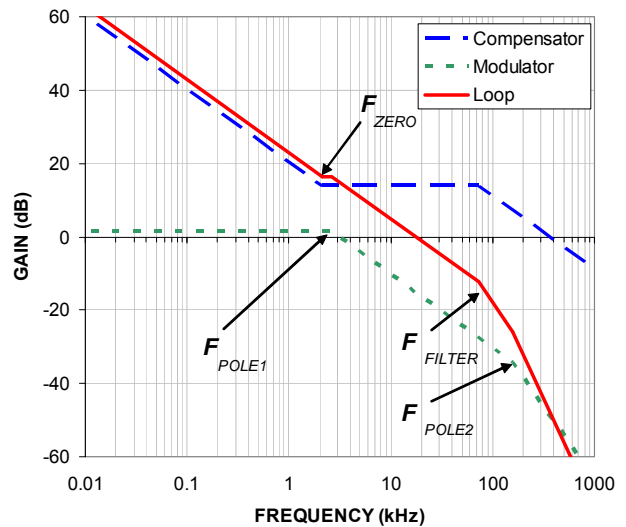


FIGURE 22. CHARGE CURRENT LOOP BODE PLOTS

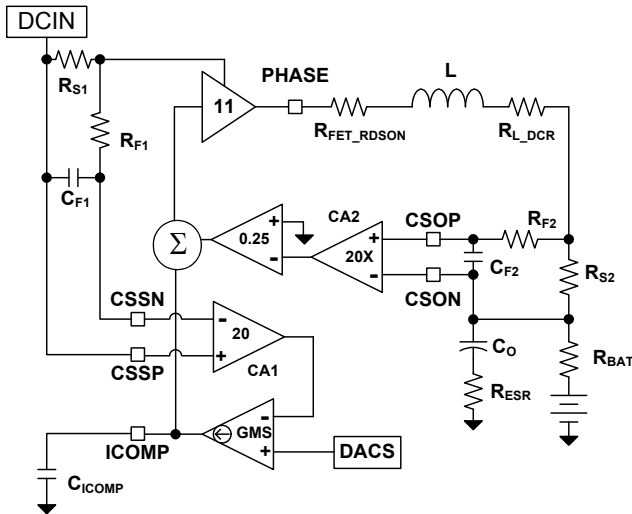


FIGURE 23. ADAPTER CURRENT LIMIT CONTROL LOOP

The loop response equations, bode plots and the selection of  $C_{ICOMP}$  are the same as the charge current control loop with loop gain reduced by the duty cycle and the ratio of  $R_{S1}/R_{S2}$ . In other words, if  $R_{S1} = R_{S2}$  and the duty cycle  $D = 50\%$ , the loop gain will be 6dB lower than the loop gain in Figure 23. This gives lower crossover frequency and higher phase margin in this mode. If  $R_{S1}/R_{S2} = 2$  and the duty cycle is 50% then the adapter current loop gain will be identical to the gain in Figure 23.

A filter should be added between  $R_{S1}$  and CSIP and CSIN to reduce switching noise. The filter roll off frequency should be between the crossover frequency and the switching frequency (~100kHz).

### Voltage Control Loop

When the battery is charged to the voltage set by ChargeVoltage register the voltage error amplifier (GMV) takes control of the output (assuming that the adapter current is below the limit set by ACLIM). The voltage error amplifier (GMV) discharges the capacitor on VCOMP to limit the output voltage. The current to the battery decreases as the cells charge to the fixed voltage and the voltage across the internal battery resistance decreases. As battery current decreases the two current error amplifiers (GMI and GMS) output their maximum current and charge the capacitor on ICOMP to its maximum voltage (limited to 0.3V above VCOMP). With high voltage on ICOMP, the minimum voltage buffer output equals the voltage on VCOMP.

The voltage control loop is shown in Figure 24.

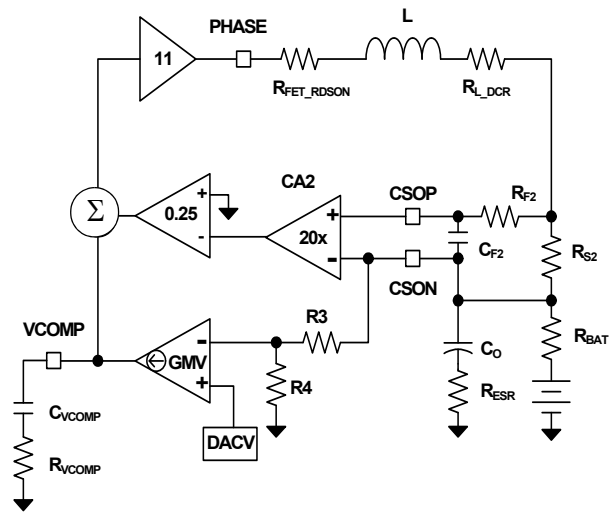


FIGURE 24. VOLTAGE CONTROL LOOP

### Output LC Filter Transfer Functions

The gain from the phase node to the system output and battery depend entirely on external components. Typical output LC filter response is shown in Figure 25. Transfer function  $A_{LC}(s)$  is shown in Equation 22:

$$A_{LC} = \frac{\left(1 - \frac{s}{\omega_{ESR}}\right)}{\left(\frac{s^2}{\omega_{DP}^2} + \frac{s}{\omega_{LC} \cdot Q} + 1\right)}$$

$$\omega_{ESR} = \frac{1}{(R_{ESR} \cdot C_0)} \quad \omega_{LC} = \frac{1}{(\sqrt{L \cdot C_0})} \quad Q = R_0 \cdot \sqrt{\frac{L}{C_0}}$$

(EQ. 22)

The resistance  $R_0$  is a combination of MOSFET  $r_{DS(ON)}$ , inductor DCR,  $R_{SENSE}$  and the internal resistance of the battery (normally between 50mΩ and 200mΩ). The worst case for voltage mode control is when the battery is absent. This results in the highest Q of the LC filter and the lowest phase margin.

The compensation network consists of the voltage error amplifier GMV and the compensation network  $R_{VCOMP}$ ,  $C_{VCOMP}$  which give the loop very high DC gain, a very low frequency pole and a zero at  $F_{ZERO1}$ . Inductor current information is added to the feedback to create a second zero  $F_{ZERO2}$ . The low pass filter  $R_{F2}$ ,  $C_{F2}$  between  $R_{S2}$  and ISL88731A add a pole at  $F_{FILTER}$ .  $R_3$  and  $R_4$  are internal divider resistors that set the DC output voltage. For a 3-cell battery,  $R_3 = 500k\Omega$  and  $R_4 = 100k\Omega$ . Equations 23 through 30 relate the compensation network's poles, zeros and gain to the components in Figure 24. Figure 26 shows an asymptotic Bode plot of the DC/DC converter's gain vs frequency. It is strongly recommended that  $F_{ZERO1}$  is approximately 30% of  $F_{LC}$  and  $F_{ZERO2}$  is approximately 70% of  $F_{LC}$ .

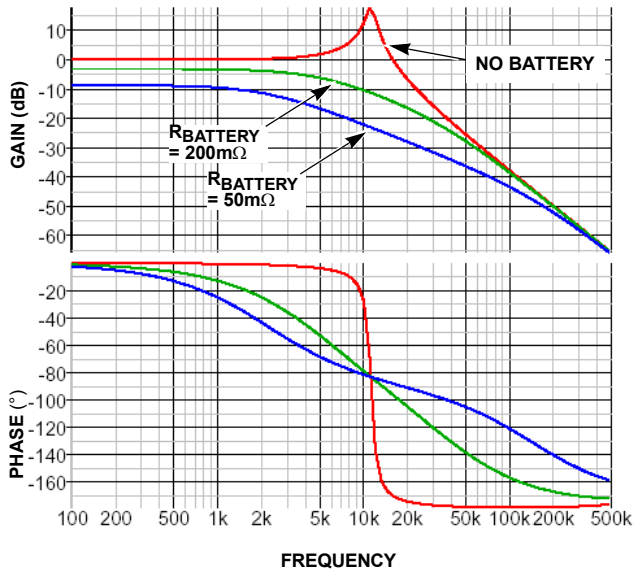


FIGURE 25. FREQUENCY RESPONSE OF THE LC OUTPUT FILTER

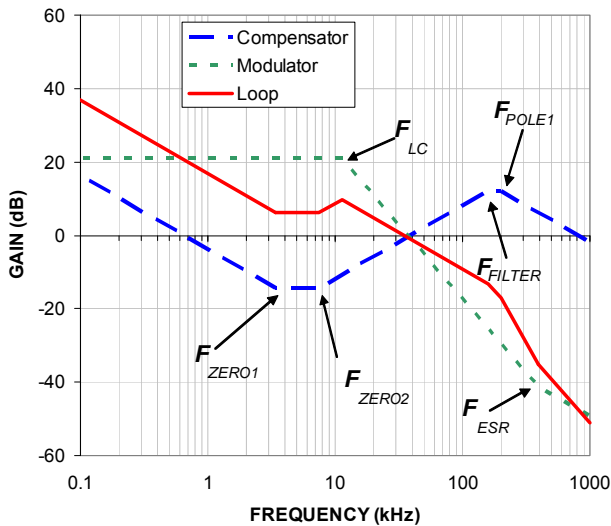


FIGURE 26. ASYMPTOTIC BODE PLOT OF THE VOLTAGE CONTROL LOOP GAIN

### Compensation Break Frequency Equations

$$F_{ZERO1} = \frac{1}{(2\pi \cdot C_{VCOMP} \cdot R_{1COMP})} \tag{EQ. 23}$$

$$F_{ZERO2} = \left( \frac{R_{VCOMP}}{2\pi \cdot R_{SENSE} \cdot C_o} \right) \cdot \left( \frac{R_4}{R_4 + R_3} \right) \cdot \left( \frac{gm1}{5} \right) \tag{EQ. 24}$$

$$F_{LC} = \frac{1}{(2\pi \sqrt{L \cdot C_o})} \tag{EQ. 25}$$

$$F_{FILTER} = \frac{1}{(2\pi \cdot R_{F2} \cdot C_{F2})} \tag{EQ. 26}$$

$$F_{POLE1} = \frac{1}{(2\pi \cdot R_{SENSE} \cdot C_o)} \tag{EQ. 27}$$

$$F_{ESR} = \frac{1}{(2\pi \cdot C_o \cdot R_{ESR})} \tag{EQ. 28}$$

Choose  $R_{VCOMP}$  equal or lower than the value calculated from Equation 29.

$$R_{VCOMP} = (0.7 \cdot F_{LC}) \cdot (2\pi \cdot C_o \cdot R_{SENSE}) \cdot \left( \frac{5}{gm1} \right) \cdot \left( \frac{R_3 + R_4}{R_4} \right) \tag{EQ. 29}$$

Next choose  $C_{VCOMP}$  equal or higher than the value calculated from Equation 30.

$$C_{VCOMP} = \frac{1}{(0.3 \cdot F_{LC}) \cdot (2\pi \cdot R_{VCOMP})} \tag{EQ. 30}$$

### PCB Layout Considerations

#### Power and Signal Layers Placement on the PCB

As a general rule, power layers should be close together, either on the top or bottom of the board, with signal layers on the opposite side of the board. As an example, layer arrangement on a 4-layer board is shown below:

1. Top Layer: signal lines, or half board for signal lines and the other half board for power lines
2. Signal Ground
3. Power Layers: Power Ground
4. Bottom Layer: Power MOSFET, Inductors and other Power traces

Separate the power voltage and current flowing path from the control and logic level signal path. The controller IC will stay on the signal layer, which is isolated by the signal ground to the power signal traces.

#### Component Placement

The power MOSFET should be close to the IC so that the gate drive signal, the LGATE, UGATE, PHASE, and BOOT, traces can be short.

Place the components in such a way that the area under the IC has less noise traces with high  $dv/dt$  and  $di/dt$ , such as gate signals and phase node signals.

## Signal Ground and Power Ground Connection

At minimum, a reasonably large area of copper, which will shield other noise couplings through the IC, should be used as signal ground beneath the IC. The best tie-point between the signal ground and the power ground is at the negative side of the output capacitor on each side, where there is little noise; a noisy trace beneath the IC is not recommended.

## GND and VCC Pin

At least one high quality ceramic decoupling capacitor should be used to cross these two pins. The decoupling capacitor can be put close to the IC.

## LGATE Pin

This is the gate drive signal for the bottom MOSFET of the buck converter. The signal going through this trace has both high  $dv/dt$  and high  $di/dt$ , and the peak charging and discharging current is very high. These two traces should be short, wide, and away from other traces. There should be no other traces in parallel with these traces on any layer.

## PGND Pin

PGND pin should be laid out to the negative side of the relevant output capacitor with separate traces. The negative side of the output capacitor must be close to the source node of the bottom MOSFET. This trace is the return path of LGATE.

## PHASE Pin

This trace should be short, and positioned away from other weak signal traces. This node has a very high  $dv/dt$  with a voltage swing from the input voltage to ground. No trace should be in parallel with it. This trace is also the return path for UGATE. Connect this pin to the high-side MOSFET source.

## UGATE Pin

This pin has a square shape waveform with high  $dv/dt$ . It provides the gate drive current to charge and discharge the top MOSFET with high  $di/dt$ . This trace should be wide, short, and away from other traces, similar to the LGATE.

## BOOT Pin

This pin's  $di/dt$  is as high as the UGATE; therefore, this trace should be as short as possible.

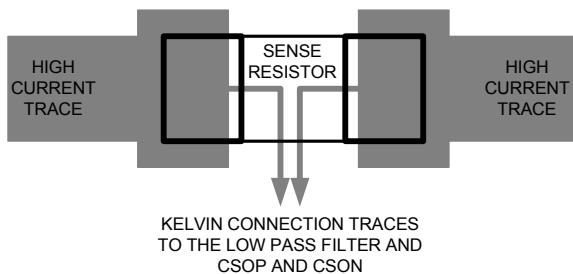


FIGURE 27. CURRENT SENSE RESISTOR LAYOUT

## CSOP, CSON, CSSP and CSSN Pins

Accurate charge current and adapter current sensing is critical for good performance. The current sense resistor connects to the CSON and the CSOP pins through a low pass filter with the filter capacitor very near the IC (see Figure 2). Traces from the sense resistor should start at the pads of the sense resistor and should be routed close together, through the low pass filter and to the CSOP and CSON pins (see Figure 27). The CSON pin is also used as the battery voltage feedback. The traces should be routed away from the high  $dv/dt$  and  $di/dt$  pins like PHASE, BOOT pins. In general, the current sense resistor should be close to the IC. These guidelines should also be followed for the adapter current sense resistor and CSSP and CSSN. Other layout arrangements should be adjusted accordingly.

## DCIN Pin

This pin connects to AC-adapter output voltage, and should be less noise sensitive.

## Copper Size for the Phase Node

The capacitance of PHASE should be kept very low to minimize ringing. It would be best to limit the size of the PHASE node copper in strict accordance with the current and thermal management of the application.

## Identify the Power and Signal Ground

The input and output capacitors of the converters, the source terminal of the bottom switching MOSFET PGND should connect to the power ground. The other components should connect to signal ground. Signal and power ground are tied together at one point.

## Clamping Capacitor for Switching MOSFET

It is recommended that ceramic capacitors be used closely connected to the drain of the high-side MOSFET, and the source of the low-side MOSFET. This capacitor reduces the noise and the power loss of the MOSFET.

**© Copyright Intersil Americas LLC 2008-2011. All Rights Reserved.**  
**All trademarks and registered trademarks are the property of their respective owners.**

For additional products, see [www.intersil.com/en/products.html](http://www.intersil.com/en/products.html)

---

Intersil products are manufactured, assembled and tested utilizing ISO9001 quality systems as noted in the quality certifications found at [www.intersil.com/en/support/qualandreliability.html](http://www.intersil.com/en/support/qualandreliability.html)

---

*Intersil products are sold by description only. Intersil may modify the circuit design and/or specifications of products at any time without notice, provided that such modification does not, in Intersil's sole judgment, affect the form, fit or function of the product. Accordingly, the reader is cautioned to verify that datasheets are current before placing orders. Information furnished by Intersil is believed to be accurate and reliable. However, no responsibility is assumed by Intersil or its subsidiaries for its use; nor for any infringements of patents or other rights of third parties which may result from its use. No license is granted by implication or otherwise under any patent or patent rights of Intersil or its subsidiaries.*

---

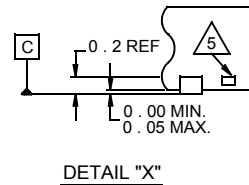
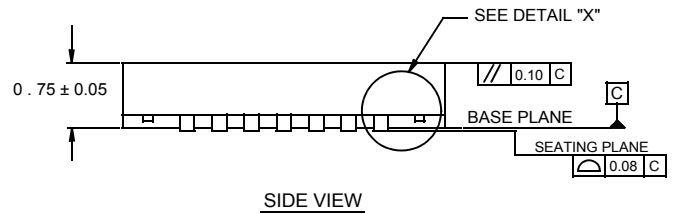
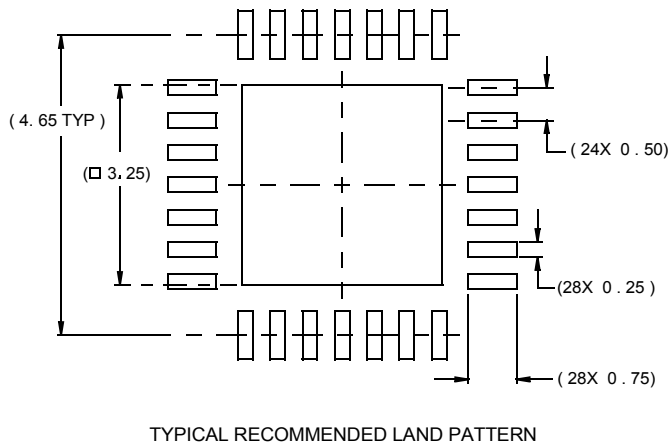
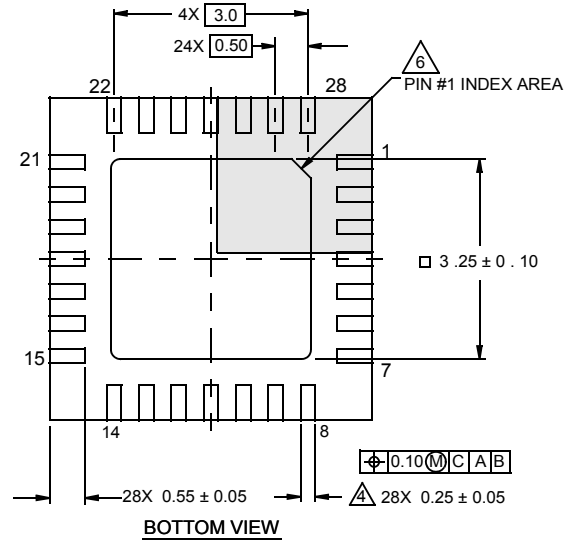
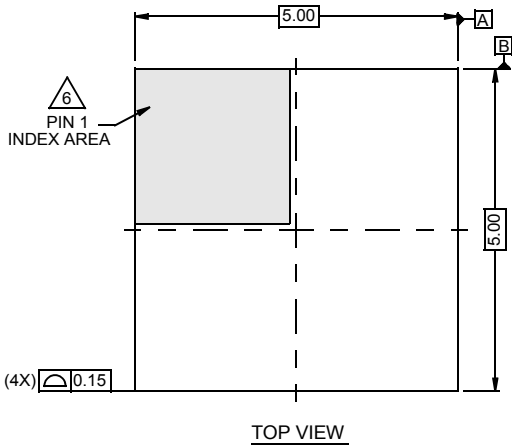
For information regarding Intersil Corporation and its products, see [www.intersil.com](http://www.intersil.com)

# Package Outline Drawing

## L28.5x5B

28 LEAD THIN QUAD FLAT NO-LEAD PLASTIC PACKAGE

Rev 1, 10/07



NOTES:

1. Dimensions are in millimeters.  
Dimensions in ( ) for Reference Only.
2. Dimensioning and tolerancing conform to AMSE Y14.5m-1994.
3. Unless otherwise specified, tolerance : Decimal ± 0.05
4. Dimension b applies to the metallized terminal and is measured between 0.15mm and 0.30mm from the terminal tip.
5. Tiebar shown (if present) is a non-functional feature.
6. The configuration of the pin #1 identifier is optional, but must be located within the zone indicated. The pin #1 identifier may be either a mold or mark feature.



Компания «Океан Электроники» предлагает заключение долгосрочных отношений при поставках импортных электронных компонентов на взаимовыгодных условиях!

Наши преимущества:

- Поставка оригинальных импортных электронных компонентов напрямую с производств Америки, Европы и Азии, а так же с крупнейших складов мира;
- Широкая линейка поставок активных и пассивных импортных электронных компонентов (более 30 млн. наименований);
- Поставка сложных, дефицитных, либо снятых с производства позиций;
- Оперативные сроки поставки под заказ (от 5 рабочих дней);
- Экспресс доставка в любую точку России;
- Помощь Конструкторского Отдела и консультации квалифицированных инженеров;
- Техническая поддержка проекта, помощь в подборе аналогов, поставка прототипов;
- Поставка электронных компонентов под контролем ВП;
- Система менеджмента качества сертифицирована по Международному стандарту ISO 9001;
- При необходимости вся продукция военного и аэрокосмического назначения проходит испытания и сертификацию в лаборатории (по согласованию с заказчиком);
- Поставка специализированных компонентов военного и аэрокосмического уровня качества (Xilinx, Altera, Analog Devices, Intersil, Interpoint, Microsemi, Actel, Aeroflex, Peregrine, VPT, Syfer, Eurofarad, Texas Instruments, MS Kennedy, Miteq, Cobham, E2V, MA-COM, Hittite, Mini-Circuits, General Dynamics и др.);

Компания «Океан Электроники» является официальным дистрибьютором и эксклюзивным представителем в России одного из крупнейших производителей разъемов военного и аэрокосмического назначения «JONHON», а так же официальным дистрибьютором и эксклюзивным представителем в России производителя высокотехнологичных и надежных решений для передачи СВЧ сигналов «FORSTAR».



## JONHON

«JONHON» (основан в 1970 г.)

Разъемы специального, военного и аэрокосмического назначения:

(Применяются в военной, авиационной, аэрокосмической, морской, железнодорожной, горно- и нефтедобывающей отраслях промышленности)

«FORSTAR» (основан в 1998 г.)

ВЧ соединители, коаксиальные кабели, кабельные сборки и микроволновые компоненты:

(Применяются в телекоммуникациях гражданского и специального назначения, в средствах связи, РЛС, а так же военной, авиационной и аэрокосмической отраслях промышленности).



Телефон: 8 (812) 309-75-97 (многоканальный)

Факс: 8 (812) 320-03-32

Электронная почта: [ocean@oceanchips.ru](mailto:ocean@oceanchips.ru)

Web: <http://oceanchips.ru/>

Адрес: 198099, г. Санкт-Петербург, ул. Калинина, д. 2, корп. 4, лит. А